Mixed-mode oscillations and interspike interval statistics in the stochastic FitzHugh-Nagumo model

Nils Berglund, Damien Landon

Mixed-mode oscillations and interspike interval statistics in the stochastic FitzHugh–Nagumo model

Nils Berglund*† and Damien Landon*†

October 13, 2011

Abstract

We study the stochastic FitzHugh–Nagumo equations, modelling the dynamics of neuronal action potentials, in parameter regimes characterised by mixed-mode oscillations. The interspike time interval is related to the random number of small-amplitude oscillations separating consecutive spikes. We prove that this number has an asymptotically geometric distribution, whose parameter is related to the principal eigenvalue of a substochastic Markov chain. We provide rigorous bounds on this eigenvalue in the small-noise regime, and derive an approximation of its dependence on the system's parameters for a large range of noise intensities. This yields a precise description of the probability distribution of observed mixed-mode patterns and interspike intervals.

Mathematical Subject Classification. 60H10, 34C26 (primary) 60J20, 92C20 (secondary)
Keywords and phrases. FitzHugh–Nagumo equations, interspike interval distribution, mixed-mode oscillation, singular perturbation, fast–slow system, dynamic bifurcation, canard, substochastic Markov chain, principal eigenvalue, quasi-stationary distribution.

1 Introduction

Deterministic conduction-based models for action-potential generation in neuron axons have been much studied for over half a century. In particular, the four-dimensional Hodgkin–Huxley equations [HH52] have been extremely successful in reproducing the observed behaviour. Of particular interest is the so-called excitable regime, when the neuron is at rest, but reacts sensitively and reliably to small external perturbations, by emitting a so-called spike. Until recently, most research efforts have been concerned with the effect of deterministic perturbations. During the last decade, however, there has been growing interest in quantifying the effect of random perturbations as well. See for instance [TP01b, TTP02, Row07] for numerical studies of the effect of noise on the interspike interval distribution in the Hodgkin–Huxley equations.

Being four-dimensional, the Hodgkin–Huxley equations are notoriously difficult to study already in the deterministic case. For this reason, several simplified models have been introduced. In particular, the two-dimensional FitzHugh–Nagumo equations [Fit55,

*MAPMO, CNRS – UMR 6628, Université d'Orléans, Fédération Denis Poisson – FR 2964, B.P. 6759, 45067 Orléans Cedex 2, France.

†Supported by ANR project MANDy, Mathematical Analysis of Neuronal Dynamics, ANR-09-BLAN-0008-01.

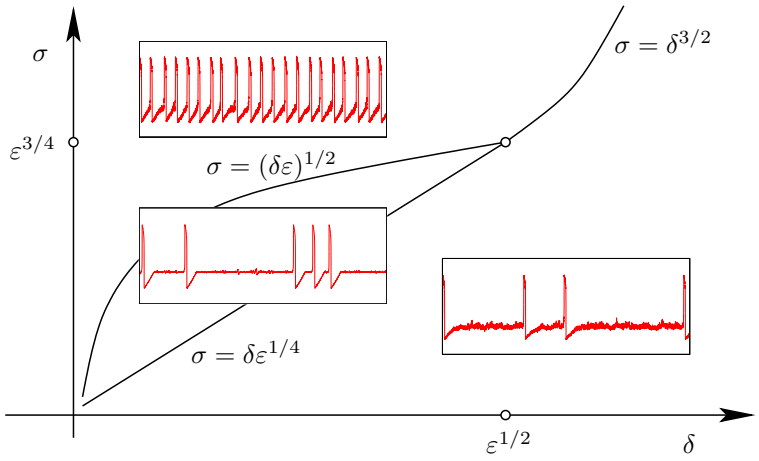

FIGURE 1. Schematic phase diagram of the stochastic FitzHugh–Nagumo equations. The parameter σ measures the noise intensity, δ measures the distance to the singular Hopf bifurcation, and ε is the timescale separation. The three main regimes are characterised be rare isolated spikes, clusters of spikes, and repeated spikes.

Fit61, NAY62], which generalise the Van der Pol equations, are able to reproduce one type of excitability, which is associated with a Hopf bifurcation (excitability of type II [Izh00]).

The effect of noise on the FitzHugh–Nagumo equations or similar excitable systems has been studied numerically [KP03, KP06, TGOS08, BKLLC11] and using moment methods [TP01a] and approximate solutions of the Fokker–Planck equations [LSG99, SK]. Rigorous results on the oscillatory (as opposed to excitable) regime have been obtained using the theory of large deviations [MVEE05, DT09] and by a detailed description of sample paths near so-called canard solutions [Sow08].

An interesting connection between excitability and mixed-mode oscillations (MMOs) was observed by Kosmidis and Pakdaman [KP03, KP06], and further analysed by Muratov and Vanden-Eijnden [MVE08]. MMOs are patterns of alternating large- and small-amplitude oscillations (SAOs), which occur in a variety of chemical and biological systems. In the deterministic case, at least three variables are necessary to reproduce such a behaviour (see [DGK+11] for a recent review of deterministic mechanisms responsible for MMOs). As observed in [KP03, KP06, MVE08], in the presence of noise, already the two-dimensional FitzHugh–Nagumo equations can display MMOs. In fact, depending on the three parameters noise intensity σ, timescale separation ε and distance to the Hopf bifurcation δ, a large variety of behaviours can be observed, including sporadic single spikes, clusters of spikes, bursting relaxation oscillations and coherence resonance. Figure 1 shows a simplified version of the phase diagram proposed in [MVE08].

In the present work, we build on ideas of [MVE08] to study in more detail the transition from rare individual spikes, through clusters of spikes and all the way to bursting relaxation oscillations. We begin by giving a precise mathematical definition of a random variable N counting the number of SAOs between successive spikes. It is related to a substochastic continuous-space Markov chain, keeping track of the amplitude of each SAO. We use this Markov process to prove that the distribution of N is asymptotically geometric, with a parameter directly related to the principal eigenvalue of the Markov chain (Theorem 3.2). A similar behaviour has been obtained for the length of bursting relaxation oscillations in a three-dimensional system [HM09]. In the weak noise regime, we derive rigorous bounds on the principal eigenvalue and on the expected number of SAOs (Theorem 4.2). Finally,

we derive an approximate expression for the distribution of N for all noise intensities up to the regime of repeated spiking (Proposition 5.1).

The rest of this paper is organised as follows. Section 2 contains the precise definition of the model. In Section 3, we define the random variable N and derive its general properties. Section 4 discusses the weak-noise regime, and Section 5 the transition from weak to strong noise. We present some numerical simulations in Section 6, and give concluding remarks in Section 7. A number of more technical computations are contained in the appendix.

Acknowledgements

It's a pleasure to thank Barbara Gentz, Simona Mancini and Khashayar Pakdaman for numerous inspiring discussions, Athanasios Batakis for advice on harmonic measures, and Christian Kuehn for sharing his deep knowledge on mixed-mode oscillations. We also thank the two anonymous referees for providing constructive remarks which helped to improve the manuscript. NB was partly supported by the International Graduate College "Stochastics and real world models" at University of Bielefeld. NB and DL thank the CRC 701 at University of Bielefeld for hospitality.

2 Model

We will consider random perturbations of the deterministic FitzHugh–Nagumo equations given by

$$\begin{aligned} \varepsilon \dot{x} &= x - x^3 + y \\ \dot{y} &= a - bx - cy \ , \end{aligned} \tag{2.1}$$

where $a, b, c \in \mathbb{R}$ and $\varepsilon > 0$ is a small parameter. The smallness of ε implies that x changes rapidly, unless the state (x, y) is close to the nullcline $\{y = x^3 - x\}$. Thus System (2.1) is called a fast-slow system, x being the fast variable and y the slow one.

We will assume that $b \neq 0$. Scaling time by a factor b and redefining the constants a, c and ε, we can and will replace b by 1 in (2.1). If $c \geqslant 0$ and c is not too large, the nullclines $\{y = x^3 - x\}$ and $\{a = x + cy\}$ intersect in a unique stationary point P. If $c < 0$, the nullclines intersect in 3 aligned points, and we let P be the point in the middle. It can be written $P = (\alpha, \alpha^3 - \alpha)$, where α satisfies the relation

$$\alpha + c(\alpha^3 - \alpha) = a \ . \tag{2.2}$$

The Jacobian matrix of the vector field at P is given by

$$J = \begin{pmatrix} \dfrac{1 - 3\alpha^2}{\varepsilon} & \dfrac{1}{\varepsilon} \\ -1 & -c \end{pmatrix} \ . \tag{2.3}$$

It has determinant $(1 - c(1 - 3\alpha^2))/\varepsilon$ and trace

$$\operatorname{Tr} J = \frac{3(\alpha_*^2 - \alpha^2)}{\varepsilon} \ , \qquad \text{where } \alpha_* = \sqrt{\frac{1 - c\varepsilon}{3}} \ . \tag{2.4}$$

Thus if $|c| < 1/\sqrt{\varepsilon}$, J admits a pair of conjugate imaginary eigenvalues when $\alpha = \pm\alpha_*$. Furthermore, the eigenvalues' real parts are of order $(\alpha_* - \alpha)/\varepsilon$ near α_*. The system undergoes so-called singular Hopf bifurcations [BE86, BE92, Bra98] at $\alpha = \pm\alpha_*$.

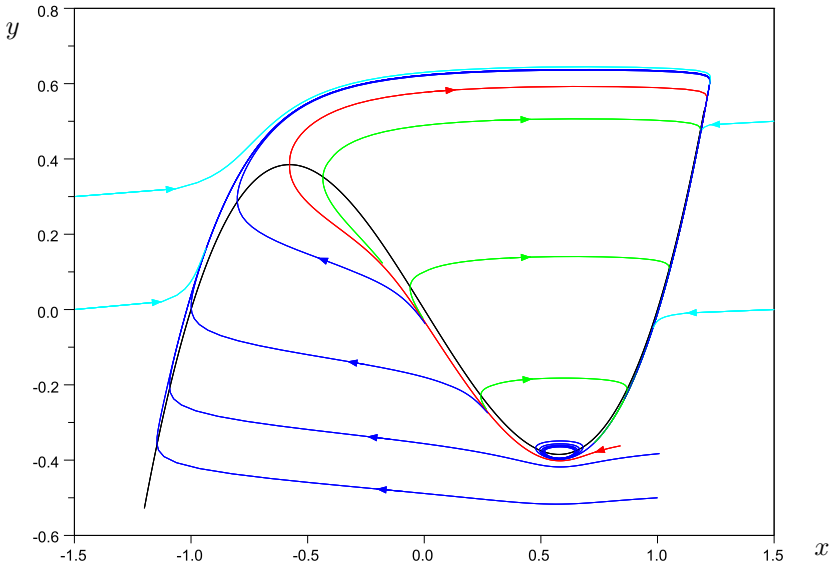

FIGURE 2. Some orbits of the deterministic FitzHugh–Nagumo equations (2.1) for parameter values $\varepsilon = 0.05$, $a = 0.58$, $b = 1$ and $c = 0$. The black curve is the nullcline, and the red orbit is the separatrix.

We are interested in the excitable regime, when $\alpha - \alpha_*$ is small and positive. In this situation, P is a stable stationary point, corresponding to a quiescent neuron. However, a small perturbation of the initial condition, e.g. a slight decrease of the y-coordinate, causes the system to make a large excursion to the region of negative x, before returning to P (Figure 2). This behaviour corresponds to a spike in the neuron's membrane potential, followed by a return to the quiescent state. One can check from the expression of the Jacobian matrix that P is a focus for $\alpha - \alpha_*$ of order $\sqrt{\varepsilon}$. Then return to rest involves small-amplitude oscillations (SAOs), of exponentially decaying amplitude.

For later use, let us fix a particular orbit delimiting the spiking and quiescent regimes, called *separatrix*. An arbitrary but convenient choice for the separatrix is the negative-time orbit of the local maximum $(-1/\sqrt{3}, 2/(3\sqrt{3}))$ of the nullcline (Figure 2). The main results will not depend on the detailed choice of the separatrix.

In this work we consider random perturbations of the deterministic system (2.1) by Gaussian white noise. They are described by the system of Itô stochastic differential equations (SDEs)

$$\begin{aligned} \mathrm{d}x_t &= \frac{1}{\varepsilon}(x_t - x_t^3 + y_t)\,\mathrm{d}t + \frac{\sigma_1}{\sqrt{\varepsilon}}\,\mathrm{d}W_t^{(1)} \\ \mathrm{d}y_t &= (a - x_t - cy_t)\,\mathrm{d}t + \sigma_2\,\mathrm{d}W_t^{(2)}\ , \end{aligned} \tag{2.5}$$

where $W_t^{(1)}$ and $W_t^{(2)}$ are independent, standard Wiener processes, and $\sigma_1, \sigma_2 > 0$. The parameter a will be our bifurcation parameter, while c is assumed to be fixed, and small enough for the system to operate in the excitable regime. The scaling in $1/\sqrt{\varepsilon}$ of the noise intensity in the first equation is chosen because the variance of the noise term then grows like $\sigma_1^2 t/\varepsilon$, so that σ_1^2 measures the ratio of diffusion and drift for the x-variable, while σ_2^2 plays the same rôle for the y-variable.

Figure 3 shows a selection of time series for the stochastic FitzHugh–Nagumo equations (2.5). For the chosen parameter values, one can clearly see large-amplitude spikes,

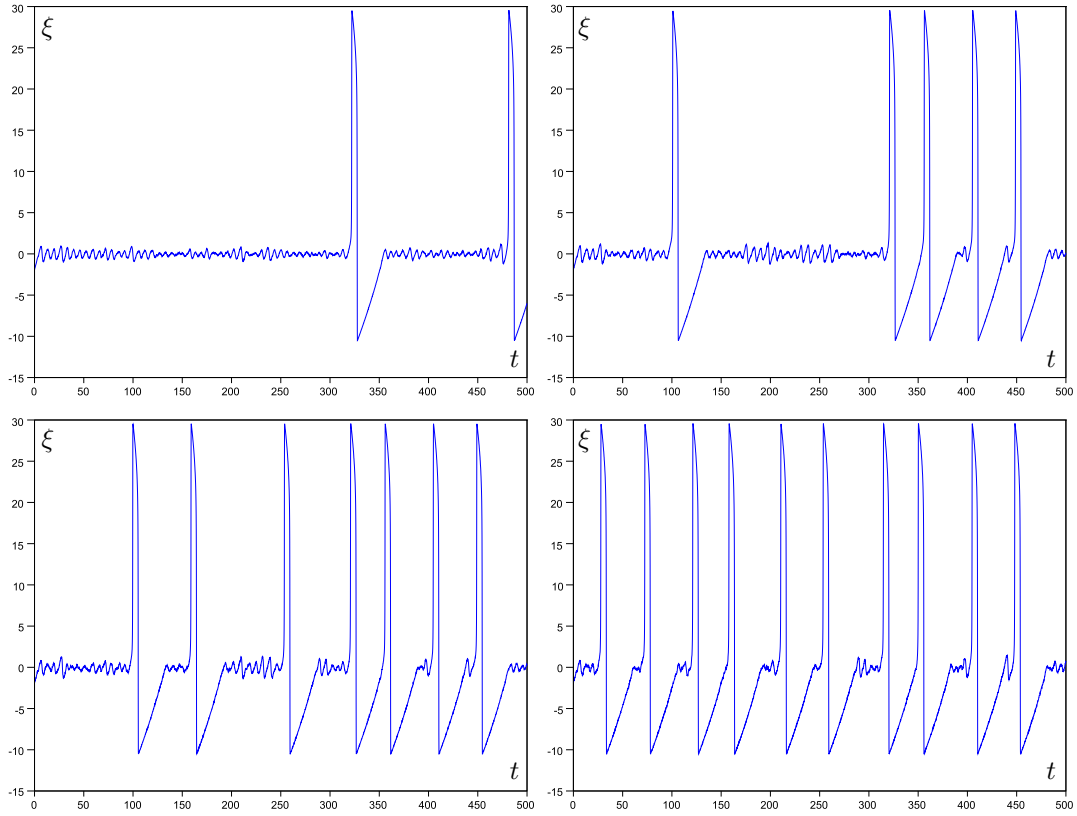

FIGURE 3. Examples of time series of the stochastic FitzHugh–Nagumo equations (2.5). The plots show the functions $t \mapsto \xi_t$, where the variable ξ is defined in Section 4. Parameter values are $\varepsilon = 0.01$ and $\delta = 3 \cdot 10^{-3}$ for the top row, $\delta = 5 \cdot 10^{-3}$ for the bottom row. The noise intensities are given by $\sigma_1 = \sigma_2 = 1.46 \cdot 10^{-4}$, $1.82 \cdot 10^{-4}$, $2.73 \cdot 10^{-4}$ and $3.65 \cdot 10^{-4}$.

separated by a random number of SAOs.

3 The distribution of small-amplitude oscillations

Let us now define an integer-valued random variable N, counting the number of small-amplitude oscillations the stochastic system performs between two consecutive spikes. The definition is going to be topological, making our results robust to changes in details of the definition. We start by fixing a bounded set $\mathcal{D} \subset \mathbb{R}^2$, with smooth boundary $\partial\mathcal{D}$, containing the stationary point P and a piece of the separatrix (Figure 4). Any excursion of the sample path $(x_t, y_t)_t$ outside $\mathcal{D}$ will be considered as a spike. N is defined as the number of times the sample path winds around P before leaving $\mathcal{D}$, and thus displaying a spike.

To define N precisely, we let $\mathcal{B}$ be a small ball of radius $\rho > 0$ centred in P. Then we draw a smooth curve $\mathcal{F}$ from $\mathcal{B}$ to the boundary $\partial\mathcal{D}$, which we parametrise by a variable $r \in [0, 1]$ proportional to arclength (the results will be independent, however, of the choice of $\mathcal{F}$ and of r). We extend the parametrisation of $\mathcal{F}$ to a polar-like parametrisation of all $\mathcal{D} \setminus \mathcal{B}$, i.e. we choose a diffeomorphism $T : [0, 1] \times \mathbb{S}^1 \to \mathcal{D}$, $(r, \varphi) \mapsto (x, y)$, where $T^{-1}(\mathcal{F}) = \{\varphi = 0\}$, $T^{-1}(\partial\mathcal{D}) = \{r = 0\}$ and $T^{-1}(\partial\mathcal{B}) = \{r = 1\}$. We also arrange that $\dot{\varphi} > 0$ near P for the deterministic flow.

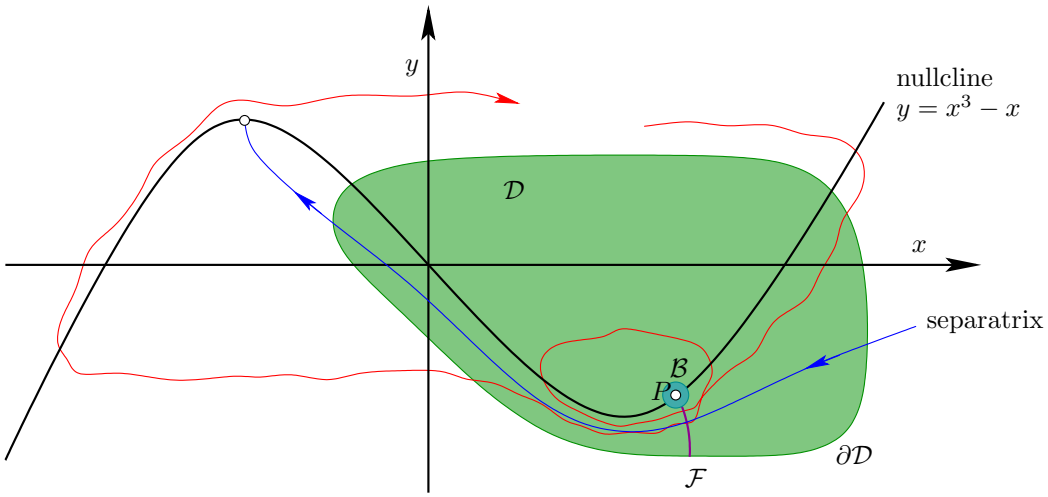

FIGURE 4. Definition of the number N of SAOs. The sample path (red) enters the region $\mathcal{D}$, and intersects twice the line $\mathcal{F}$ before leaving $\mathcal{D}$, making another spike. Thus $N = 2$ in this example. The separatrix is represented in blue.

Consider the process $(r_t, \varphi_t)_t$ (where the angle φ has been lifted from $\mathbb{S}^1$ to $\mathbb{R}$). Given an initial condition $(r_0, 0) \in T^{-1}(\mathcal{F})$ and an integer $M \geqslant 1$, we define the stopping time

$$\tau = \inf\{t > 0 \colon \varphi_t \in \{2\pi, -2M\pi\} \text{ or } r_t \in \{0, 1\}\} \,. \tag{3.1}$$

There are four cases to consider:

- The case $r_\tau = 0$ corresponds to the sample path (x_t, y_t) leaving $\mathcal{D}$, and thus to a spike. This happens with strictly positive probability, by ellipticity of the diffusion process (2.5). In this situation, we set by convention $N = 1$.
- In the case $\varphi_\tau = 2\pi$ and $r_\tau \in (0, 1)$, the sample path has returned to $\mathcal{F}$ after performing a complete revolution around P, staying all the while in $\mathcal{D} \setminus \mathcal{B}$. This corresponds to an SAO, and thus $N \geqslant 2$.
- The case $r_\tau = 1$ corresponds to the sample path entering $\mathcal{B}$, which we consider as the neuron reaching the quiescent state. In that case we simply wait until the state leaves $\mathcal{B}$ again and either hits $\mathcal{F}$ or leaves $\mathcal{D}$.
- The case $\varphi_\tau = -2M\pi$ and $r_\tau \in (0, 1)$ represents the (unlikely) event that the sample path winds M time around P in the wrong direction. We introduce this case for technical reasons only, as we will need τ to be the first-exit time of a bounded set. For simplicity, we also consider this situation as one SAO.

As long as $r_\tau \in (0, 1)$, we repeat the above procedure, incrementing N at each iteration. This yields a sequence $(R_0, R_1, \dots, R_{N-1})$ of random variables, describing the position of the successive intersections of the path with $\mathcal{F}$, separated by rotations around P, and up to the first exit from $\mathcal{D}$.

Remark 3.1. The above definition of N is the simplest one to analyse mathematically. There are several possible alternatives. One can, for instance, introduce a quiescent state $(x, y) \in \mathcal{B}$, and define N as the number of SAOs until the path either leaves $\mathcal{D}$ or enters $\mathcal{B}$. This would allow to keep track of the number of SAOs between successive spikes and/or quiescent phases. Another possibility would be to count rotations in both the positive and negative directions. For simplicity, we stick here to the above simplest definition of N, but we plan to make a more refined study in a future work.

The sequence $(R_n)_n$ forms a substochastic Markov chain on $E = (0, 1)$, with kernel

$$K(R, A) = \mathbb{P}\big\{\varphi_\tau = 2\pi, r_\tau \in A \;\big|\; \varphi_0 = 0, r_0 = R\big\}\,, \qquad R \in E, A \subset E \text{ a Borel set}\,. \quad (3.2)$$

The Markov chain is substochastic because $K(R, E) < 1$, due to the positive probability of sample paths leaving $\mathcal{D}$. We can make it stochastic in the usual way by adding a cemetery state Δ to E (the spike), and setting $K(R, \Delta) = 1 - K(R, E)$, $K(\Delta, \Delta) = 1$ (see [Ore71, Num84] for the general theory of such processes).

The number of SAOs is given by

$$N = \inf\big\{n \geqslant 1\colon R_n = \Delta\big\} \in \mathbb{N} \cup \{\infty\} \quad (3.3)$$

(we set $\inf \emptyset = \infty$). A suitable extension of the well-known Perron–Frobenius theorem (see [Jen12, KR50, Bir57]) shows that K admits a maximal eigenvalue λ_0, which is real and simple. It is called the *principal eigenvalue* of K. If there exists a probability measure π_0 such that $\pi_0 K = \lambda_0 \pi_0$, it is called the *quasi-stationary distribution (QSD)* of the kernel K [SVJ66].

Our first main result gives qualitative properties of the distribution of N valid in all parameter regimes with nonzero noise.

Theorem 3.2 (General properties of N)**.** *Assume that $\sigma_1, \sigma_2 > 0$. Then for any initial distribution μ_0 of R_0 on the curve $\mathcal{F}$,*

- *the kernel K admits a quasi-stationary distribution π_0;*
- *the associated principal eigenvalue $\lambda_0 = \lambda_0(\varepsilon, a, c, \sigma_1, \sigma_2)$ is strictly smaller than 1;*
- *the random variable N is almost surely finite;*
- *the distribution of N is "asymptotically geometric", that is,*

$$\lim_{n\to\infty} \mathbb{P}^{\mu_0}\big\{N = n + 1 \;\big|\; N > n\big\} = 1 - \lambda_0\,; \quad (3.4)$$

- *$\mathbb{E}^{\mu_0}\left\{r^N\right\} < \infty$ for $r < 1/\lambda_0$ and thus all moments $\mathbb{E}^{\mu_0}\left\{N^k\right\}$ of N are finite.*

Proof: Let us denote by $K(x, \mathrm{d}y)$ the kernel defined in (3.2). We consider K as a bounded linear operator on $L^\infty(E)$, acting on bounded measurable functions by

$$f(x) \mapsto (Kf)(x) = \int_E K(x, \mathrm{d}y) f(y) = \mathbb{E}^x\left\{f(R_1)\right\}\,, \quad (3.5)$$

and as a bounded linear operator on $L^1(E)$, acting on finite measures μ by

$$\mu(A) \mapsto (\mu K)(A) = \int_E \mu(\mathrm{d}x) K(x, A) = \mathbb{P}^\mu\{R_1 \in A\}\,. \quad (3.6)$$

To prove existence of a QSD π_0, we first have to establish a uniform positivity condition on the kernel. Note that in $K(x, \mathrm{d}y)$, y represents the first-exit location from the domain $\mathcal{G} = (0, 1) \times (-2M\pi, 2\pi)$, for an initial condition $(x, 0)$, in case the exit occurs through one of the lines $\varphi = -2M\pi$ or $\varphi = 2\pi$. In harmonic analysis, $K(x, \mathrm{d}y)$ is called the harmonic measure for the generator of the diffusion in $\mathcal{G}$ based at $(x, 0)$. In the case of Brownian motion, it has been proved in [Dah77] that sets of positive Hausdorff measure have positive harmonic measure. This result has been substantially extended in [BAKS84], where the authors prove that for a general class of hypoelliptic diffusions, the harmonic measure admits a smooth density $k(x, y)$ with respect to Lebesgue measure $\mathrm{d}y$. Our diffusion

process being uniformly elliptic for $\sigma_1, \sigma_2 > 0$, it enters into the class of processes studied in that work. Specifically, [BAKS84, Corollary 2.11] shows that $k(x, y)$ is smooth, and its derivatives are bounded by a function of the distance from x to y. This distance being uniformly bounded below by a positive constant in our setting, there exists a constant $L \in \mathbb{R}_+$ such that

$$\frac{\sup_{y \in E} k(x, y)}{\inf_{y \in E} k(x, y)} \leqslant L \qquad \forall x \in E \,. \tag{3.7}$$

We set

$$s(x) = \inf_{y \in E} k(x, y) \,. \tag{3.8}$$

Then it follows that

$$s(x) \leqslant k(x, y) \leqslant L s(x) \qquad \forall x, y \in E \,. \tag{3.9}$$

Thus the kernel K fulfils the uniform positivity condition

$$s(x)\nu(A) \leqslant K(x, A) \leqslant L s(x)\nu(A) \qquad \forall x \in E \,, \forall A \subset E \tag{3.10}$$

for ν given by the Lebesgue measure. It follows by [Bir57, Theorem 3] that K admits unique positive left and right unit eigenvectors, and that the corresponding eigenvalue λ_0 is real and positive. In other words, there is a measure π_0 and a positive function h_0 such that $\pi_0 K = \lambda_0 \pi_0$ and $K h_0 = \lambda_0 h_0$. We normalise the eigenvectors in such a way that

$$\pi_0(E) = \int_E \pi_0(\mathrm{d}x) = 1 \,, \qquad \pi_0 h_0 = \int_E \pi_0(\mathrm{d}x) h_0(x) = 1 \,. \tag{3.11}$$

Thus π_0 is indeed the quasistationary distribution of the Markov chain. Notice that

$$\lambda_0 = \lambda_0 \pi_0(E) = \int_E \pi_0(\mathrm{d}x) K(x, E) \leqslant \pi_0(E) = 1 \,, \tag{3.12}$$

with equality holding if and only if $K(x, E) = 1$ for π_0-almost all $x \in E$. In our case, $K(x, E) < 1$ since E has strictly smaller Lebesgue measure than $\partial\mathcal{G}$, and the density of the harmonic measure is bounded below. This proves that $\lambda_0 < 1$.

Lemma 3 in [Bir57] shows that for any bounded measurable function $f : E \to \mathbb{R}$, there exists a finite constant $M(f)$ such that the spectral-gap estimate

$$|(K^n f)(x) - \lambda_0^n (\pi_0 f) h_0(x)| \leqslant M(f)(\lambda_0 \rho)^n h_0(x) \tag{3.13}$$

holds for some $\rho < 1$ (note that this confirms that λ_0 is indeed the leading eigenvalue of K). In order to prove that N is almost surely finite, we first note that

$$\mathbb{P}^{\mu_0}\big\{N > n\big\} = \mathbb{P}^{\mu_0}\big\{R_n \in E\big\} = \int_E \mu_0(\mathrm{d}x) K^n(x, E) \,. \tag{3.14}$$

Applying (3.13) with $f = \mathbf{1}$, the function identically equal to 1, we obtain

$$\lambda_0^n h_0(x) - M(\mathbf{1})(\lambda_0 \rho)^n h_0(x) \leqslant K^n(x, E) \leqslant \lambda_0^n h_0(x) + M(\mathbf{1})(\lambda_0 \rho)^n h_0(x) \,. \tag{3.15}$$

Integrating against μ_0, we get

$$\lambda_0^n \big(1 - M(\mathbf{1})\rho^n\big) \leqslant \mathbb{P}^{\mu_0}\big\{N > n\big\} \leqslant \lambda_0^n \big(1 + M(\mathbf{1})\rho^n\big) \,. \tag{3.16}$$

Since $\lambda_0 < 1$, it follows that $\lim_{n\to\infty} \mathbb{P}^{\mu_0}\{N > n\} = 0$, i.e., N is almost surely finite.

In order to prove that N is asymptotically geometric, we have to control

$$\mathbb{P}^{\mu_0}\big\{N = n+1\big\} = \int_E \int_E \mu_0(\mathrm{d}x) K^n(x, \mathrm{d}y)\big[1 - K(y, E)\big] \; . \tag{3.17}$$

Applying (3.13) with $f(y) = 1 - K(y, E)$, and using the fact that

$$\pi_0 f = 1 - \int_E \pi_0(\mathrm{d}y) K(y, E) = 1 - \lambda_0 \tag{3.18}$$

yields

$$\lambda_0^n\big(1 - \lambda_0 - M(f)\rho^n\big) \leqslant \mathbb{P}^{\mu_0}\big\{N = n+1\big\} \leqslant \lambda_0^n\big(1 - \lambda_0 + M(f)\rho^n\big) \; . \tag{3.19}$$

Hence (3.4) follows upon dividing (3.19) by (3.16) and taking the limit $n \to \infty$.

Finally, the moment generating function $\mathbb{E}^{\mu_0}\big\{r^N\big\}$ can be represented as follows:

$$\begin{aligned} \mathbb{E}^{\mu_0}\big\{r^N\big\} &= \sum_{n\geqslant 0} r^n \mathbb{P}^{\mu_0}\big\{N = n\big\} = \sum_{n\geqslant 0}\Big[1 + (r-1)\sum_{m=0}^{n-1} r^m\Big]\mathbb{P}^{\mu_0}\big\{N = n\big\} \\ &= 1 + (r-1)\sum_{m\geqslant 0} r^m \mathbb{P}^{\mu_0}\big\{N > m\big\} \; , \end{aligned} \tag{3.20}$$

which converges for $|r\lambda_0| < 1$ as a consequence of (3.16). □

Note that in the particular case where the initial distribution μ_0 is equal to the QSD π_0, the random variable R_n has the law $\mu_n = \lambda_0^n \pi_0$, and N follows an exponential law of parameter $1 - \lambda_0$:

$$\mathbb{P}^{\pi_0}\big\{N = n\big\} = \lambda_0^{n-1}(1 - \lambda_0) \qquad \text{and} \qquad \mathbb{E}^{\pi_0}\big\{N\big\} = \frac{1}{1 - \lambda_0} \; . \tag{3.21}$$

In general, however, the initial distribution μ_0 after a spike will be far from the QSD π_0, and thus the distribution of N will only be asymptotically geometric.

Theorem 3.2 allows to quantify the clusters of spikes observed in [MVE08]. To this end, we have to agree on a definition of clusters of spikes. One may decide that a cluster is a sequence of successive spikes between which there is no complete SAO, i.e. $N = 1$ between consecutive spikes. If the time resolution is not very good, however, one may also fix a threshold SAO number $n_0 \geqslant 1$, and consider as a cluster a succession of spikes separated by at most n_0 SAOs. Let $\mu_0^{(n)}$ be the arrival distribution on $\mathcal{F}$ of sample paths after the nth spike. Then the probability to observe a cluster of length k is given by

$$\mathbb{P}^{\mu_0^{(0)}}\big\{N \leqslant n_0\big\}\mathbb{P}^{\mu_0^{(1)}}\big\{N \leqslant n_0\big\} \dots \mathbb{P}^{\mu_0^{(k-1)}}\big\{N \leqslant n_0\big\}\mathbb{P}^{\mu_0^{(k)}}\big\{N > n_0\big\} \; . \tag{3.22}$$

In general, the consecutive spikes will not be independent, and thus the distributions $\mu_0^{(n)}$ will be different. For small noise, however, after a spike sample paths strongly concentrate near the stable branch of the nullcline (see the discussion in [BG09, Section 3.5.2]), and thus we expect all $\mu_0^{(n)}$ to be very close to some constant distribution μ_0. This implies that the lengths of clusters of spikes also follow an approximately geometric distribution :

$$\mathbb{P}\big\{\text{cluster of length } k\big\} \simeq p^k(1-p) \qquad \text{where } p = \mathbb{P}^{\mu_0}\big\{N \leqslant n_0\big\} \; . \tag{3.23}$$

4 The weak-noise regime

In order to obtain more quantitative results, we start by transforming the FitzHugh-Nagumo equations to a more suitable form. The important part of dynamics occurs near the singular Hopf bifurcation point. We carry out the transformation in four steps, the first two of which have already been used in [BE86, BE92] :

1. An affine transformation $x = \alpha_* + u$, $y = \alpha_*^3 - \alpha_* + v$ translates the origin to the bifurcation point, and yields, in the deterministic case (2.1), the system
$$\begin{aligned} \varepsilon \dot{u} &= v + c\varepsilon u - 3\alpha_* u^2 - u^3 \ , \\ \dot{v} &= \delta - u - cv \ , \end{aligned} \tag{4.1}$$
where $\delta = a - \alpha_* - c(\alpha_*^3 - \alpha_*)$ is small and positive. Note that (2.2) implies that δ is of order $\alpha - \alpha_*$ near the bifurcation point, and thus measures the distance to the Hopf bifurcation. In particular, by (2.4) the eigenvalues of the Jacobian matrix J have real parts of order $-\delta/\varepsilon$.
2. The scaling of space and time given by $u = \sqrt{\varepsilon}\xi$, $v = \varepsilon\eta$ and $t = \sqrt{\varepsilon}t'$ yields
$$\begin{aligned} \dot{\xi} &= \eta - 3\alpha_*\xi^2 + \sqrt{\varepsilon}\big(c\xi - \xi^3\big) \ , \\ \dot{\eta} &= \frac{\delta}{\sqrt{\varepsilon}} - \xi - \sqrt{\varepsilon}\, c\eta \ , \end{aligned} \tag{4.2}$$
where dots now indicate derivation with respect to t'. On this scale, the nullcline $\dot{\xi} = 0$ is close to the parabola $\eta = 3\alpha_*\xi^2$.
3. The nonlinear transformation $\eta = 3\alpha_*\xi^2 + z - 1/(6\alpha_*)$ has the effect of straightening out the nullcline, and transforms (4.2) into
$$\begin{aligned} \dot{\xi} &= z - \frac{1}{6\alpha_*} + \sqrt{\varepsilon}\big(c\xi - \xi^3\big) \ , \\ \dot{z} &= \frac{\delta}{\sqrt{\varepsilon}} - 6\alpha_*\xi z + \sqrt{\varepsilon}\bigg(6\alpha_*\xi^4 + c\Big(\frac{1}{6\alpha_*} - 9\alpha_*\xi^2 - z\Big)\bigg) \ . \end{aligned} \tag{4.3}$$
4. Finally, we apply the scaling $\xi \mapsto -\xi/3\alpha_*$, $z \mapsto z/3\alpha_*$, which yields
$$\begin{aligned} \dot{\xi} &= \frac{1}{2} - z + \sqrt{\varepsilon}\bigg(c\xi - \frac{1}{9\alpha_*^2}\xi^3\bigg) \ , \\ \dot{z} &= \mu + 2\xi z + \sqrt{\varepsilon}\bigg(\frac{2}{9\alpha_*^2}\xi^4 + c\Big(\frac{1}{2} - 3\xi^2 - z\Big)\bigg) \ , \end{aligned} \tag{4.4}$$
where the distance to the Hopf bifurcation is now measured by the parameter
$$\mu = \frac{3\alpha_*\delta}{\sqrt{\varepsilon}} \ . \tag{4.5}$$
If we neglect the terms of order $\sqrt{\varepsilon}$ in (4.4), we obtain a very simple system, with a stationary point at $(-\mu, 1/2)$. If in addition $\mu = 0$, the line $z = 0$ is invariant. Orbits starting in $\{z < 0\}$ go to $-\infty$ (which corresponds to a spike), while orbits starting in $\{z > 0\}$ rotate around the stationary point (making an SAO). Thus $\{z = 0\}$ is indeed the separatrix in that limit. Figure 5 shows some orbits in a case with slightly positive μ, when the separatrix lies in the region $\{z < 0\}$.

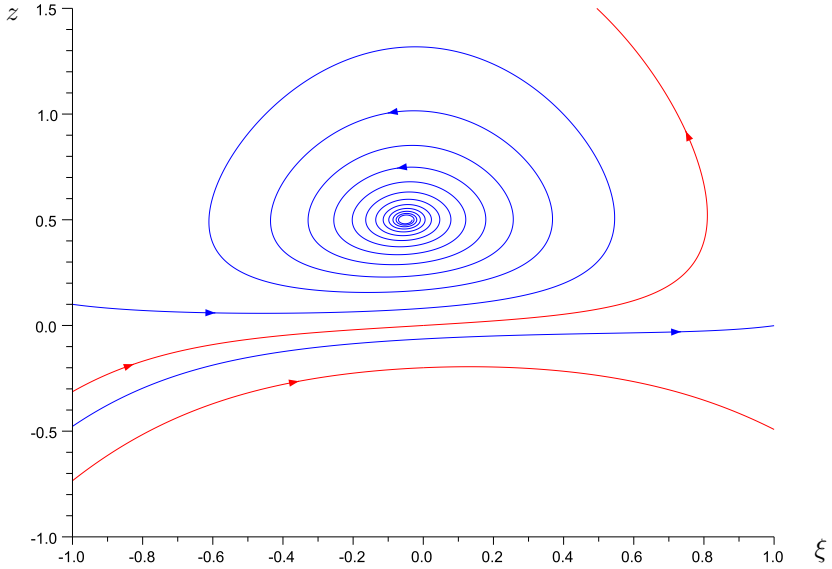

FIGURE 5. Some orbits of the deterministic equations (4.4) in (ξ, z)-coordinates, for parameter values $\varepsilon = 0.01$, $\mu = 0.05$ and $c = 0$ (i.e. $\alpha_* = 1/\sqrt{3}$).

Carrying out the same transformations for the stochastic system (2.5) yields the following result (we omit the proof, which is a straightforward application of Itô's formula).

Proposition 4.1. *In the new variables (ξ, z), and on the new timescale $t/\sqrt{\varepsilon}$, the stochastic FitzHugh–Nagumo equations (2.5) take the form*

$$\begin{aligned} \mathrm{d}\xi_t &= \left[\frac{1}{2} - z_t + \sqrt{\varepsilon}\Big(c\xi_t - \frac{1}{9\alpha_*^2}\xi_t^3\Big)\right]\mathrm{d}t + \tilde{\sigma}_1\,\mathrm{d}W_t^{(1)}\,, \\ \mathrm{d}z_t &= \left[\tilde{\mu} + 2\xi_t z_t + \sqrt{\varepsilon}\Big(\frac{2}{9\alpha_*^2}\xi_t^4 + c\Big(\frac{1}{2} - 3\xi_t^2 - z_t\Big)\Big)\right]\mathrm{d}t - 2\tilde{\sigma}_1\xi_t\,\mathrm{d}W_t^{(1)} + \tilde{\sigma}_2\,\mathrm{d}W_t^{(2)}\,, \end{aligned} \tag{4.6}$$

where

$$\begin{aligned} \tilde{\sigma}_1 &= -3\alpha_*\varepsilon^{-3/4}\sigma_1\,, \\ \tilde{\sigma}_2 &= 3\alpha_*\varepsilon^{-3/4}\sigma_2\,, \\ \tilde{\mu} &= \mu - \tilde{\sigma}_1^2 = \frac{3\alpha_*(\delta - 3\alpha_*\sigma_1^2/\varepsilon)}{\sqrt{\varepsilon}}\,. \end{aligned} \tag{4.7}$$

When z is close to 0, the dynamics of z_t is dominated by two terms : the term $\tilde{\mu}\,\mathrm{d}t$, which pushes sample paths upwards to the region of SAOs, and the noise terms. We can thus expect that if $\tilde{\sigma}_1^2 + \tilde{\sigma}_2^2 \ll \tilde{\mu}^2$, then the upwards drift dominates, and the system will make many SAOs between two consecutive spikes. Going back to original parameters, the condition translates into $\sigma_1^2 + \sigma_2^2 \ll (\varepsilon^{1/4}\delta)^2$.

Making these ideas rigorous, we obtain the following theorem.

Theorem 4.2 (Weak-noise regime)**.** *Assume that ε and $\delta/\sqrt{\varepsilon}$ are sufficiently small. If $c \neq 0$, assume further that $\delta \geqslant |c|\varepsilon^\beta$ for some $\beta > 1$. Then there exists a constant $\kappa > 0$ such that for $\sigma_1^2 + \sigma_2^2 \leqslant (\varepsilon^{1/4}\delta)^2/\log(\sqrt{\varepsilon}/\delta)$, the principal eigenvalue λ_0 satisfies*

$$1 - \lambda_0 \leqslant \exp\left\{-\kappa\frac{(\varepsilon^{1/4}\delta)^2}{\sigma_1^2 + \sigma_2^2}\right\}. \tag{4.8}$$

Furthermore, for any initial distribution μ_0 of incoming sample paths, the expected number of SAOs satisfies

$$\mathbb{E}^{\mu_0}\big\{N\big\} \geqslant C(\mu_0)\exp\left\{\kappa\frac{(\varepsilon^{1/4}\delta)^2}{\sigma_1^2+\sigma_2^2}\right\}. \tag{4.9}$$

Here $C(\mu_0)$ is the probability that the incoming path hits $\mathcal{F}$ above the separatrix.

PROOF: The result follows of we can prove the existence of a subset $A \subset E$ with positive Lebesgue measure that the Markov chain is unlikely to leave. Indeed, let

$$\varepsilon_A = \sup_{x\in A}\big[1-K(x,A)\big] \tag{4.10}$$

be the maximal probability to leave A when starting in A. Let us show that

$$\lambda_0 \geqslant 1-\varepsilon_A\,. \tag{4.11}$$

Indeed, the relation $\lambda_0\pi_0 = \pi_0 K$ yields

$$\begin{aligned}\lambda_0\pi_0(A) &= \int_A \pi_0(\mathrm{d}x)K(x,A) + \int_{E\setminus A}\pi_0(\mathrm{d}x)K(x,A)\\ &\geqslant \pi_0(A)(1-\varepsilon_A) + \int_{E\setminus A}\pi_0(\mathrm{d}x)s(x)\,\nu(A)\,.\end{aligned} \tag{4.12}$$

Either $\pi_0(A)=1$, and the result follows immediately. Or $\pi_0(A)<1$, and thus $\pi_0(E\setminus A)>0$, so that the second term on the right-hand side is strictly positive. It follows that $\lambda_0\pi_0(A)>0$, and we obtain (4.11) upon dividing by $\pi_0(A)$.

Next, let us prove that

$$\mathbb{E}^{\mu_0}\{N\} \geqslant \frac{\mu_0(A)}{\varepsilon_A}\,. \tag{4.13}$$

For $x\in A$, let $\theta(x) = \mathbb{E}^x\{N\} = \sum_{n\geqslant 0}K^n(x,E)$. Then $\theta(x) = \lim_{n\to\infty}\theta_n(x)$ where

$$\theta_n(x) = \sum_{m=0}^{n} K^m(x,E)\,. \tag{4.14}$$

We have

$$\theta_{n+1}(x) = 1 + (K\theta_n)(x) \geqslant 1 + \int_A K(x,\mathrm{d}y)\theta_n(y)\,. \tag{4.15}$$

Now let $m_n = \inf_{x\in A}\theta_n(x)$. Then $m_0=1$ and

$$m_{n+1} \geqslant 1 + (1-\varepsilon_A)m_n\,. \tag{4.16}$$

By induction on n we get

$$m_n \geqslant \frac{1}{\varepsilon_A} - \frac{(1-\varepsilon_A)^{n+1}}{\varepsilon_A}\,, \tag{4.17}$$

so that $\mathbb{E}^x\{N\} = \theta(x) \geqslant 1/\varepsilon_A$ for all $x\in A$, and (4.13) follows upon integrating against μ_0 over A.

It thus remains to construct a set $A\subset E$ such that ε_A is exponentially small in $\tilde{\mu}^2/(\tilde{\sigma}_1^2+\tilde{\sigma}_2^2)$. The detailed computations being rather involved, we give them in the

appendix, and only summarise the main steps here. We first have to choose the curve $\mathcal{F}$ defining the Markov chain. Let us introduce two broken lines

$$F_- = \Big\{\xi = -L \text{ and } z \leqslant \frac{1}{2}\Big\} \cup \Big\{-L \leqslant \xi \leqslant 0 \text{ and } z = \frac{1}{2}\Big\} \tag{4.18}$$

and

$$F_+ = \Big\{\xi = L \text{ and } z \leqslant \frac{1}{2}\Big\} \cup \Big\{0 \leqslant \xi \leqslant L \text{ and } z = \frac{1}{2}\Big\}\,, \tag{4.19}$$

where the parameter L is given by

$$L^2 = \frac{\gamma}{2}\big(-\log(c_-\tilde{\mu})\big)\,, \tag{4.20}$$

where $c_- > 0$ and $\gamma > 0$ are adjustable constants. The curve $\mathcal{F}$ will correspond to the broken line F_-, while F_+ allows to split the computations into two distinct steps.

1. In the first step, we take an initial condition $(-L, z_0)$ on F_-, with z_0 of order $\tilde{\mu}^{1-\gamma}$. It is easy to show that the deterministic solution starting in $(-L, z_0)$ hits F_+ for the first time at a point $z_T^0 \geqslant c_0\tilde{\mu}^{1-\gamma}$ where $c_0 > 0$. Consider now the stochastic sample path starting in $(-L, z_0)$. Proposition A.4 in Appendix A shows that there are constants $C, \kappa_1 > 0$ such that the sample path hits F_+ for the first time at a point (L, z_1) satisfying
$$\mathbb{P}\big\{z_1 < c_0\tilde{\mu}^{1-\gamma} - \tilde{\mu}\big\} \leqslant \frac{C}{\tilde{\mu}^{2\gamma}}\,\mathrm{e}^{-\kappa_1\tilde{\mu}^2/\tilde{\sigma}^2}\ . \tag{4.21}$$
This is done by first approximating (4.6) by a linear system, and then showing that the effect of nonlinear terms is small.
2. In the second step, we show that a sample path starting in $(L, z_1) \in F_+$ returns with high probability to F_- at a point $(-L, z_0')$ with $z_0' \geqslant z_1$. The coordinates (ξ, z) are not well adapted to this part of the dynamics, because z is likely to become very large and ξ is not monotonous. The idea, already used in [MVE08], is to draw on the fact that the variable
$$Q = 2z\,\mathrm{e}^{-2z-2\xi^2+1} \tag{4.22}$$
is a constant of motion in the deterministic case, when $\tilde{\mu} = 0$. Thus by introducing an angle variable ϕ such that the change of variables $(\xi, z) \mapsto (\phi, Q)$ is well-defined in the region of interest, and using an averaging procedure, we can show that Q varies little between F_+ and F_-. Corollary B.5 in Appendix B shows that there is a $\kappa_2 > 0$ such that
$$\mathbb{P}\big\{z_0' < z_1 \,\big|\, z_1 \geqslant c_0\tilde{\mu}^{1-\gamma} - \tilde{\mu}\big\} \leqslant 2\,\mathrm{e}^{-\kappa_2\tilde{\mu}^2/\tilde{\sigma}^2}\ . \tag{4.23}$$

In the above results, we assume that either $c = 0$, or $c \neq 0$ and $\tilde{\mu}^{1+\theta} \geqslant \sqrt{\varepsilon}$ for some $\theta > 0$. The reason is that if $c = 0$, we can draw on the fact that the error terms of order $\sqrt{\varepsilon}$ in (4.6) are positive, while if $c \neq 0$ we only know their order. Choosing A as the set of points in F_- for which $z \geqslant c_0\tilde{\mu}^{1-\gamma} - \tilde{\mu}$, we obtain that ε_A is bounded by the sum of (4.21) and (4.23), and the results follow by returning to original parameters. □

Relation (4.9) shows that the average number of SAOs between two consecutive spikes is exponentially large in this regime. Note that each SAO requires a rescaled time of order 1 (see Section B.1), and thus a time of order $\sqrt{\varepsilon}$ in original units. It follows that the average interspike interval length is obtained by multiplying (4.9) by a constant times $\sqrt{\varepsilon}$.

Relation (3.4) shows that the distribution of N is asymptotically geometric with parameter given by (4.8). Hence the interspike interval distribution will be close to an exponential one, but with a periodic modulation due to the SAOs.

5 The transition from weak to strong noise

We now give an approximate description of how the dynamics changes with increasing noise intensity. Assume that we start (4.6) with an initial condition (ξ_0, z_0) where $\xi_0 = -L$ for some $L > 0$ and z_0 is small. As long as z_t remains small, we may approximate ξ_t in the mean by $\xi_0 + t/2$, and thus z_t will be close to the solution of

$$\mathrm{d}z_t^1 = \Bigl(\tilde{\mu} + tz_t^1\Bigr)\,\mathrm{d}t - \tilde{\sigma}_1 t\,\mathrm{d}W_t^{(1)} + \tilde{\sigma}_2\,\mathrm{d}W_t^{(2)}\;. \tag{5.1}$$

This linear equation can be solved explicitly. In particular, at time $T = 4L$, ξ_t is close to L and we have the following result.

Proposition 5.1. *Let $2L^2 = \gamma|\log(c_-\tilde{\mu})|$ for some $\gamma, c_- > 0$. Then for any H,*

$$\mathbb{P}\bigl\{z_T^1 \leqslant -H\bigr\} = \Phi\left(-\pi^{1/4}\frac{\tilde{\mu}}{\tilde{\sigma}}\biggl[1 + \mathcal{O}\Bigl((H+z_0)\tilde{\mu}^{\gamma-1}\Bigr)\biggr]\right)\;, \tag{5.2}$$

where $\tilde{\sigma}^2 = \tilde{\sigma}_1^2 + \tilde{\sigma}_2^2$ and $\Phi(x) = \int_{-\infty}^x \mathrm{e}^{-u^2/2}\,\mathrm{d}u/\sqrt{2\pi}$ is the distribution function of the standard normal law.

Proof: Solving (5.1) by variation of the constant yields

$$z_T^1 = z_0 + \mathrm{e}^{T^2/2}\biggl[\tilde{\mu}\int_{t_0}^T \mathrm{e}^{-s^2/2}\,\mathrm{d}s - \tilde{\sigma}_1\int_{t_0}^T s\,\mathrm{e}^{-s^2/2}\,\mathrm{d}W_s^{(1)} + \tilde{\sigma}_2\int_{t_0}^T \mathrm{e}^{-s^2/2}\,\mathrm{d}W_s^{(2)}\biggr]\;. \tag{5.3}$$

Note that by the choice of L, we have $\mathrm{e}^{T^2/2} = \mathrm{e}^{2L^2} = (c_-\tilde{\mu})^{-\gamma}$. The random variable z_T^1 is Gaussian, with expectation

$$\mathbb{E}\bigl\{z_T^1\bigr\} = z_0 + \tilde{\mu}\,\mathrm{e}^{2L^2}\int_{-2L}^{2L}\mathrm{e}^{-s^2/2}\,\mathrm{d}s \tag{5.4}$$

and variance

$$\mathrm{Var}(z_T^1) = \tilde{\sigma}_1^2\,\mathrm{e}^{4L^2}\int_{-2L}^{2L} s^2\,\mathrm{e}^{-s^2}\,\mathrm{d}s + \tilde{\sigma}_2^2\,\mathrm{e}^{4L^2}\int_{-2L}^{2L}\mathrm{e}^{-s^2}\,\mathrm{d}s\;. \tag{5.5}$$

Using this in the relation

$$\mathbb{P}\bigl\{z_T^1 \leqslant -H\bigr\} = \int_{-\infty}^{-H}\frac{\mathrm{e}^{-(z-\mathbb{E}\{z_T^1\})^2/2\,\mathrm{Var}(z_T^1)}}{\sqrt{2\pi\,\mathrm{Var}(z_T^1)}}\,\mathrm{d}z = \Phi\left(-\frac{H + \mathbb{E}\{z_T^1\}}{\sqrt{\mathrm{Var}(z_T^1)}}\right) \tag{5.6}$$

yields the result. □

Choosing γ large enough, the right-hand side of (5.2) is approximately constant for a large range of values of z_0 and H. The probability that the system performs no complete SAO before spiking again should thus behave as

$$\mathbb{P}^{\mu_0}\bigl\{N = 1\bigr\} \simeq \Phi\left(-\pi^{1/4}\frac{\tilde{\mu}}{\tilde{\sigma}}\right) = \Phi\left(-\frac{(\pi\varepsilon)^{1/4}(\delta - 3\alpha_*\sigma_1^2/\varepsilon)}{\sqrt{\sigma_1^2+\sigma_2^2}}\right)\;. \tag{5.7}$$

Since $1 - \lambda_0$ is equal to the probability of leaving $\mathcal{D}$ before completing the first SAO, when starting in the QSD π_0, we expect that $1 - \lambda_0$ has a similar behaviour, provided π_0 is concentrated near $z = 0$. We can identify three regimes, depending on the value of $\tilde{\mu}/\tilde{\sigma}$:

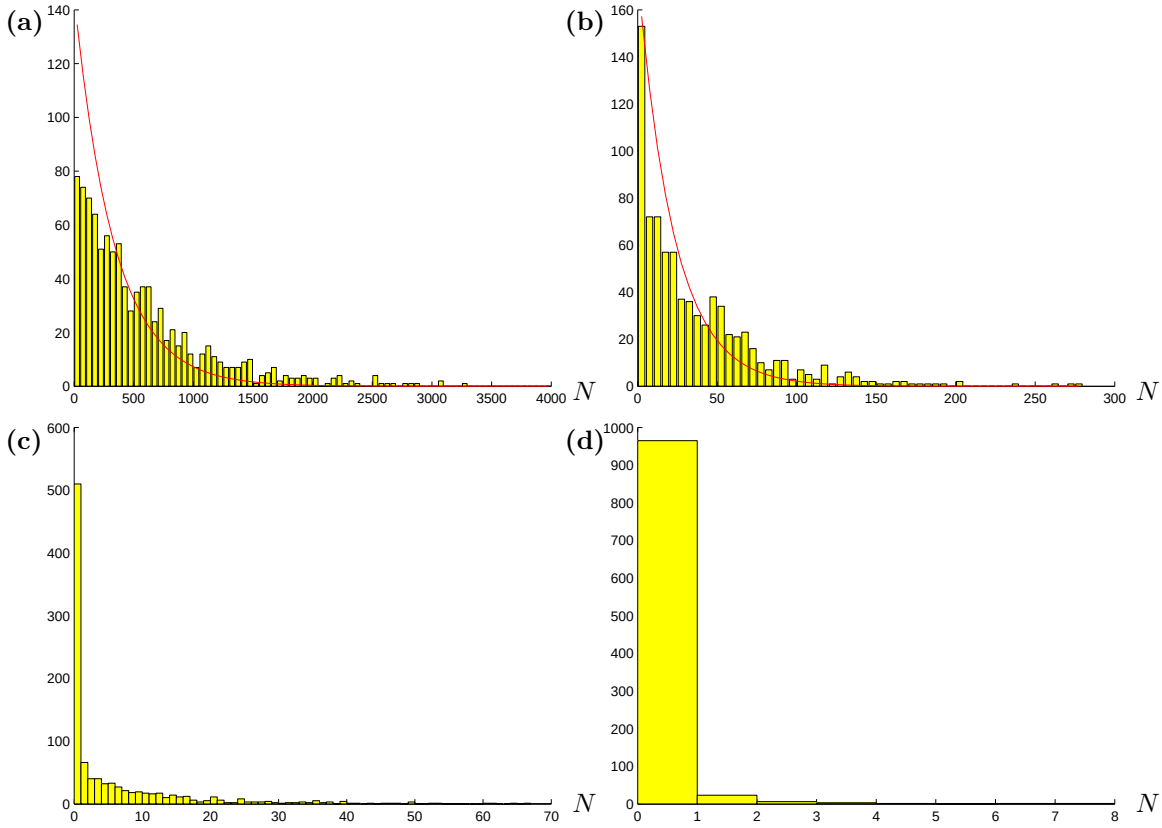

FIGURE 6. Histograms of numerically simulated distributions of the SAO number N, obtained from time series containing 1000 spikes each. The superimposed curves show geometric distributions with parameter λ_0, where λ_0 has been estimated from the expectation of r^N, as explained in the text. Parameter values are $\varepsilon = 10^{-4}$ and $\tilde{\sigma} = 0.1$ in all cases, and **(a)** $\tilde{\mu} = 0.12$, **(b)** $\tilde{\mu} = 0.05$, **(c)** $\tilde{\mu} = 0.01$, and **(d)** $\tilde{\mu} = -0.09$ (cf. (4.7) for their definition).

1. **Weak noise :** $\tilde{\mu} \gg \tilde{\sigma}$, which in original variables translates into $\sqrt{\sigma_1^2 + \sigma_2^2} \ll \varepsilon^{1/4}\delta$. This is the weak-noise regime already studied in the previous section, in which λ_0 is exponentially close to 1, and thus spikes are separated by long sequences of SAOs.
2. **Strong noise :** $\tilde{\mu} \ll -\tilde{\sigma}$, which implies $\mu \ll \tilde{\sigma}^2$, and in original variables translates into $\sqrt{\sigma_1^2 + \sigma_2^2} \gg \varepsilon^{3/4}$. Then $\mathbb{P}\{N > 1\}$ is exponentially small, of order $\mathrm{e}^{-(\sigma_1^2+\sigma_2^2)/\varepsilon^{3/2}}$. Thus with high probability, there will be no complete SAO between consecutive spikes, i.e., the neuron is spiking repeatedly.
3. **Intermediate noise :** $|\tilde{\mu}| = \mathcal{O}(\tilde{\sigma})$, which translates into $\varepsilon^{1/4}\delta \leqslant \sqrt{\sigma_1^2 + \sigma_2^2} \leqslant \varepsilon^{3/4}$. Then the mean number of SAOs is of order 1. In particular, when $\sigma_1 = \sqrt{\varepsilon\delta}$, $\tilde{\mu} = 0$ and thus $\mathbb{P}\{N = 1\}$ is close to $1/2$.

An interesting point is that the transition from weak to strong noise is gradual, being characterised by a smooth change of the distribution of N as a function of the parameters. There is no clear-cut transition at the parameter value $\sigma_1 = \sqrt{\varepsilon\delta}$ obtained in [MVE08] (cf. Figure 1), the only particularity of this parameter value being that $\mathbb{P}\{N = 1\}$ is close to $1/2$. The definition of a boundary between the intermediate and strong-noise regimes mainly depends on how well the SAOs can be resolved in time. A very good time resolution would put the boundary at noise intensities of order $\varepsilon^{3/4}$, while a lower time resolution

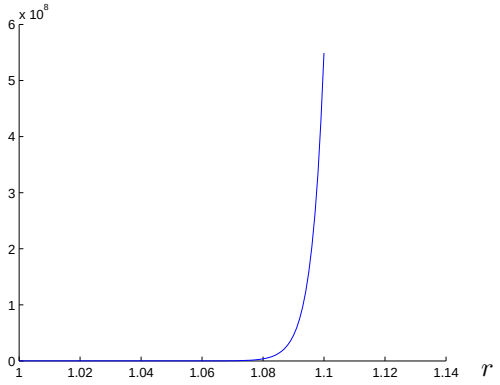

FIGURE 7. Empirical expectation of r^N as a function of r, for $\tilde{\mu} = 0.05$, $\tilde{\sigma} = 0.1$ and $\varepsilon = 10^{-4}$. The location of the pole allows to estimate $1/\lambda_0$.

would move in closer to $\sqrt{\varepsilon\delta}$.

6 Numerical simulations

Figure 6 shows numerically simulated distributions of the SAO number. The geometric decay is clearly visible. In addition, for decreasing values of $\tilde{\mu}/\tilde{\sigma}$, there is an increasing bias towards the first peak $N = 1$, which with our convention corresponds to the system performing no complete SAO between consecutive spikes. Of course this does not contradict the asymptotic result (3.4), but it shows that transient effects are important.

Due to the finite sample size, the number of events in the tails of the histograms is too small to allow for a chi-squared adequacy test. We can, however, estimate the principal eigenvalue λ_0, by using the fact that the moment generating function $\mathbb{E}^{\mu_0}\left\{r^N\right\}$ has a simple pole at $r = 1/\lambda_0$ (see (3.16) and (3.20)). Figure 7 shows an example of the dependence of the empirical expectation of r^N on r. By detecting when its derivative exceeds a given threshold, one obtains an estimate of $1/\lambda_0$. Geometric distributions with parameter λ_0 have been superimposed on two histograms in Figure 6.

Figure 8 shows, as a function of $-x = -\tilde{\mu}/\tilde{\sigma}$, the curve $x \mapsto \Phi(-\pi^{1/4}x)$, as well as the inverse of the empirical expectation of N, the probability that $N = 1$, and $1 - \lambda_0$ where the principal eigenvalue λ_0 has been estimated from the generating function. The data points for $\tilde{\mu} > 0$ have been obtained from histograms containing 1000 spikes, while those for $\tilde{\mu} < 0$ have been obtained from histograms containing 500 spikes separated by $N > 1$ SAOs (the number of spiking events with $N = 1$ being much larger). Theorem 4.2 applies to the far left of the figure, when $\tilde{\mu} \gg \tilde{\sigma}$.

As predicted by (5.7), $\mathbb{P}\{N = 1\}$ is indeed close to the theoretical value $\Phi(-\pi^{1/4}\tilde{\mu}/\tilde{\sigma})$. Recall from (3.21) that $1/\mathbb{E}^{\mu_0}\{N\}$, $\mathbb{P}^{\mu_0}\{N = 1\}$ and $1 - \lambda_0$ would be equal if the initial distribution μ_0 after a spike were equal to the QSD π_0. The simulations show that $1/\mathbb{E}\{N\}$ and $1 - \lambda_0$ are systematically smaller than $\mathbb{P}\{N = 1\}$. The difference between $\mathbb{P}\{N = 1\}$ and $1 - \lambda_0$ is a measure of how far away μ_0 is from the QSD π_0. The difference between $1/\mathbb{E}\{N\}$ and $1 - \lambda_0$ also depends on the spectral gap between λ_0 and the remaining spectrum of the Markov kernel. Note that $1/\mathbb{E}\{N\}$ and $1 - \lambda_0$ seem to follow a similar curve as $\mathbb{P}\{N = 1\}$, but with a shifted value of $\tilde{\mu}$. We do not have any explanation for this at the moment.

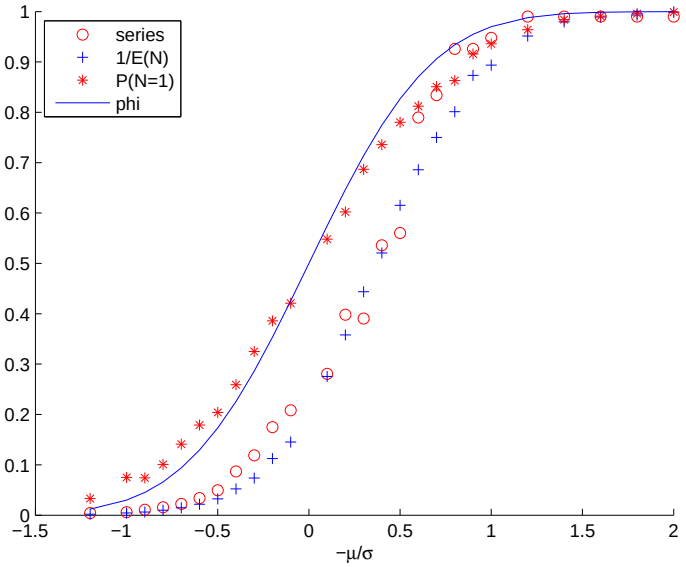

FIGURE 8. Plots of the function $\Phi(-\pi^{1/4}\tilde{\mu}/\tilde{\sigma})$ as a function of $-\tilde{\mu}/\tilde{\sigma}$ (full line), and numerical estimates of $\mathbb{P}\{N=1\}$ (stars), $1/\mathbb{E}\{N\}$ (crosses) and $1-\lambda_0$ (circles).

7 Conclusion and outlook

We have shown that in the excitable regime, and when the stationary point P is a focus, the interspike interval statistics of the stochastic FitzHugh–Nagumo equations can be characterised in terms of the random number of SAOs N. The distribution of N is asymptotically geometric, with parameter $1-\lambda_0$, where λ_0 is the principal eigenvalue of a substochastic Markov chain, describing a random Poincaré map. This result is in fact fairly general, as it does not depend at all on the details of the system. It only requires the deterministic system to admit an invariant region where the dynamics involves (damped) oscillations, so that a Poincaré section can be defined in a meaningful way. Thus Theorem 3.2 will hold true for a large class of such systems.

To be useful for applications, this qualitative result has to be complemented by quantitative estimates of the relevant parameters. Theorem 4.2 provides such estimates for λ_0 and the expected number of SAOs in the weak-noise regime $\sigma_1^2+\sigma_2^2 \ll (\varepsilon^{1/4}\delta)^2$. We have obtained one-sided estimates on these quantities, which follow from the construction of an almost invariant region A for the Markov chain. It is possible to obtain two-sided estimates by deriving more precise properties for the Markov chain, in particular a lower bound on the probability of leaving the complement of A. We expect the exponent $(\varepsilon^{1/4}\delta)^2/(\sigma_1^2+\sigma_2^2)$ to be sharp in the case $\delta \gg \varepsilon$, since this corresponds to the drift $\tilde{\mu}$ in the expression (4.6) for $\dot{z}$ dominating the error terms of order $\sqrt{\varepsilon}$ due to higher-order nonlinear terms. For smaller δ, however, there is a competition between the two terms, the effect of which is not clear and has to be investigated in more detail. The same problem prevents us from deriving any bounds for $\delta \leqslant \varepsilon$ when the parameter c defining the FitzHugh–Nagumo equations is different from zero. It may be possible to achieve a better control on the nonlinear terms by additional changes of variables.

For intermediate and strong noise, we obtained an approximation (5.7) for the probability $\mathbb{P}\{N=1\}$ of spiking immediately, showing that the transition from rare to frequent spikes is governed by the distribution function Φ of the normal law. Though we didn't

obtain rigorous bounds on the principal eigenvalue and expected number of SAOs in this regime, simulations show a fairly good agreement with the approximation for $\mathbb{P}\{N = 1\}$. The results on the Markov kernel contained in the appendix should in fact yield more precise information on λ_0 and the law of N, via approximations for the quasistationary distribution π_0. Generally speaking, however, we need better tools to approximate QSDs, principal eigenvalues and the spectral gap of substochastic Markov chains.

Finally, let us note that the approach presented here should be applicable to other excitable systems involving oscillations. For instance, for some parameter values, the Morris–Lecar equations [ML81] admit a stable stationary point surrounded by an unstable and a stable periodic orbit. In a recent work [DG11], Ditlevsen and Greenwood have combined this fact and results on linear oscillatory systems with noise to relate the spike statistics to those of an integrate-and-fire model. It would be interesting to implement the Markov-chain approach in this situation as well.

A Dynamics near the separatrix

The appendix contains some of the more technical computations required for the proof of Theorem 4.2. We treat separately the dynamics near the separatrix, and during the remainder of an SAO.

In this section, we use the equations in (ξ, z)-variables given by (4.6) to describe the dynamics in a neighbourhood of the separatrix. To be more specific, we will assume that z is small, of the order of some power of μ, and that ξ varies in an interval $[-L, L]$, where the parameter L is given by (4.20). Let $F_\pm$ be the two broken lines defined in (4.18) and (4.19). Given an initial condition $(-L, z_0) \in F_-$, our goal is to estimate where the sample path starting in $(-L, z_0)$ hits F_+ for the first time. This will characterise the first part of the Markov kernel K.

A.1 The linearised process

Before analysing the full dynamics of (4.6) we consider some approximations of the system. The fact that $\xi_t \simeq \xi_0 + t/2$ for small z motivates the change of variable

$$\xi = \frac{t}{2} + u \;, \tag{A.1}$$

which transforms the system (4.6) into

$$\begin{aligned} \mathrm{d}u_t &= \bigl(-z_t + \mathcal{O}(\tilde{\varepsilon})\bigr)\,\mathrm{d}t + \tilde{\sigma}_1\,\mathrm{d}W_t^{(1)} \;, \\ \mathrm{d}z_t &= \bigl(\tilde{\mu} + tz_t + 2u_t z_t + \mathcal{O}(\tilde{\varepsilon})\bigr)\,\mathrm{d}t - \tilde{\sigma}_1 t\,\mathrm{d}W_t^{(1)} - 2\tilde{\sigma}_1 u_t\,\mathrm{d}W_t^{(1)} + \tilde{\sigma}_2\,\mathrm{d}W_t^{(2)} \;, \end{aligned} \tag{A.2}$$

where we write $\tilde{\varepsilon} = \sqrt{\varepsilon}(L^4 + cL^2)$. We choose an initial condition $(0, z_0)$ at time $t_0 = -2L$. As a first approximation, consider the deterministic system

$$\begin{aligned} \mathrm{d}u_t^0 &= -z_t^0\,\mathrm{d}t \;, \\ \mathrm{d}z_t^0 &= \bigl(\tilde{\mu} + tz_t^0\bigr)\,\mathrm{d}t \;. \end{aligned} \tag{A.3}$$

The solution of the second equation is given by

$$z_t^0 = \mathrm{e}^{t^2/2}\biggl[z_0\,\mathrm{e}^{-t_0^2/2} + \tilde{\mu}\int_{t_0}^t \mathrm{e}^{-s^2/2}\,\mathrm{d}s\biggr] \;. \tag{A.4}$$

In particular, at time $T = 2L$, we have $\xi_T = L + u_t \simeq L$ and the location of the first-hitting point of F_+ is approximated by

$$z_T^0 = z_0 + \tilde{\mu}\, \mathrm{e}^{T^2/2} \int_{t_0}^{T} \mathrm{e}^{-s^2/2}\, \mathrm{d}s = z_0 + \mathcal{O}(\tilde{\mu}^{1-\gamma}) \,. \tag{A.5}$$

As a second approximation, we incorporate the noise terms and consider the linear SDE

$$\begin{aligned} \mathrm{d}u_t^1 &= -z_t^1\, \mathrm{d}t + \tilde{\sigma}_1\, \mathrm{d}W_t^{(1)} \,, \\ \mathrm{d}z_t^1 &= \big(\tilde{\mu} + t z_t^1\big)\, \mathrm{d}t - \tilde{\sigma}_1 t\, \mathrm{d}W_t^{(1)} + \tilde{\sigma}_2\, \mathrm{d}W_t^{(2)} \,. \end{aligned} \tag{A.6}$$

Let us now quantify the deviation between (u_t^1, z_t^1) and (u_t^0, z_t^0).

Proposition A.1. *Let*

$$\zeta(s) = \mathrm{e}^{s^2} \bigg[\mathrm{e}^{-t_0^2} + \int_{t_0}^{s} \mathrm{e}^{-u^2}\, \mathrm{d}u \bigg] \,. \tag{A.7}$$

Then there exists a constant $M > 0$ such that for all $t \geqslant t_0$, all $h, h_1, h_2 > 0$ and all $\rho \in (0, \tilde{\mu}^{2\gamma}/M)$,

$$\mathbb{P}\bigg\{ \sup_{t_0 \leqslant s \leqslant t} \frac{|z_s^1 - z_s^0|}{\sqrt{\zeta(s)}} \geqslant h \bigg\} \leqslant \frac{2(t-t_0)}{\rho} \exp\bigg\{ -\frac{1}{8} \frac{h^2}{\tilde{\sigma}^2} \big(1 - M\rho\, \tilde{\mu}^{-2\gamma}\big) \bigg\} \tag{A.8}$$

and

$$\begin{aligned} &\mathbb{P}\bigg\{ \sup_{t_0 \leqslant s \leqslant t} |u_s^1 - u_s^0| \geqslant h_1 + h_2 \int_{t_0}^{t} \sqrt{\zeta(s)}\, \mathrm{d}s \bigg\} \\ &\qquad \leqslant 2 \exp\bigg\{ -\frac{h_1^2}{2(t-t_0)\tilde{\sigma}_1^2} \bigg\} + \frac{2(t-t_0)}{\rho} \exp\bigg\{ -\frac{1}{8} \frac{h_2^2}{\tilde{\sigma}^2} \big(1 - M\rho\, \tilde{\mu}^{-2\gamma}\big) \bigg\} \,. \end{aligned} \tag{A.9}$$

Proof: The difference $(x^1, y^1) = (u^1 - u^0, z^1 - z^0)$ satisfies the system

$$\begin{aligned} \mathrm{d}x_t^1 &= -y_t^1\, \mathrm{d}t + \tilde{\sigma}_1\, \mathrm{d}W_t^{(1)} \,, \\ \mathrm{d}y_t^1 &= t\, y_t^1\, \mathrm{d}t - \tilde{\sigma}_1 t\, \mathrm{d}W_t^{(1)} + \tilde{\sigma}_2\, \mathrm{d}W_t^{(2)} \,. \end{aligned} \tag{A.10}$$

The second equation admits the solution

$$y_t^1 = \tilde{\sigma}_2\, \mathrm{e}^{t^2/2} \int_{t_0}^{t} \mathrm{e}^{-s^2/2}\, \mathrm{d}W_s^{(2)} - \tilde{\sigma}_1\, \mathrm{e}^{t^2/2} \int_{t_0}^{t} s e^{-s^2/2}\, \mathrm{d}W_s^{(1)} =: y_t^{1,1} + y_t^{1,2} \,. \tag{A.11}$$

We first estimate $y_t^{1,1}$. Let $u_0 = t_0 < u_1 < \cdots < u_K = t$ be a partition of $[t_0, t]$. The Bernstein-like estimate [BG02, Lemma 3.2] yields the bound

$$\mathbb{P}\bigg\{ \sup_{t_0 \leqslant s \leqslant t} \frac{1}{\sqrt{\zeta(s)}} \tilde{\sigma}_2 \bigg| \int_{t_0}^{s} \mathrm{e}^{(s^2-u^2)/2}\, \mathrm{d}W_u \bigg| \geqslant H_0 \bigg\} \leqslant 2 \sum_{k=1}^{K} P_k \tag{A.12}$$

for any $H_0 > 0$, where

$$P_k \leqslant \exp\bigg\{ -\frac{1}{2} \frac{H_0^2}{\tilde{\sigma}_2^2} \inf_{u_{k-1} \leqslant s \leqslant u_k} \frac{\zeta(s)}{\zeta(u_k)}\, \mathrm{e}^{u_k^2 - s^2} \bigg\} \,. \tag{A.13}$$

The definition of $\zeta(s)$ implies

$$\frac{\zeta(s)}{\zeta(u_k)}\,\mathrm{e}^{u_k^2-s^2} = 1 - \frac{1}{\zeta(u_k)}\int_s^{u_k} \mathrm{e}^{u_k^2-u^2}\,\mathrm{d}u \geqslant 1 - \int_s^{u_k} \mathrm{e}^{t_0^2-u^2}\,\mathrm{d}u\;. \tag{A.14}$$

Note that $\mathrm{e}^{t_0^2} = \mathrm{e}^{4L^2} = \mathcal{O}(\tilde{\mu}^{-2\gamma})$. For a uniform partition given by $u_k - u_{k-1} = \rho$ with $\rho \ll \tilde{\mu}^{2\gamma}$, we can bound this last expression below by

$$1 - M\rho\,\tilde{\mu}^{-2\gamma} \tag{A.15}$$

for some constant M. This yields

$$\mathbb{P}\biggl\{\sup_{0\leqslant s\leqslant t}\frac{|y_s^{1,1}|}{\sqrt{\zeta(s)}} \geqslant H_0\biggr\} \leqslant \frac{2(t-t_0)}{\rho}\exp\biggl\{-\frac{1}{2}\frac{H_0^2}{\tilde{\sigma}_2^2}\bigl(1 - M\rho\,\tilde{\mu}^{-2\gamma}\bigr)\biggr\}\;. \tag{A.16}$$

Doing the same for $y_s^{1,2}$ we obtain

$$\mathbb{P}\biggl\{\sup_{0\leqslant s\leqslant t}\frac{|y_s^{1,2}|}{\sqrt{\zeta(s)}} \geqslant H_1\biggr\} \leqslant \frac{2(t-t_0)}{\rho}\exp\biggl\{-\frac{1}{2}\frac{H_1^2}{\tilde{\sigma}_1^2}\bigl(1 - M\rho\,\tilde{\mu}^{-2\gamma}\bigr)\biggr\} \tag{A.17}$$

for any $H_1 > 0$. Letting $h = H_0 + H_1$ with $H_0 = H_1 = h/2$, we obtain (A.8). Now we can express x_t^1 in terms of y_t^1 by

$$x_t^1 = -\int_{t_0}^t y_s^1\,\mathrm{d}s + \tilde{\sigma}_1\int_{t_0}^t \mathrm{d}W_s^{(1)}\;. \tag{A.18}$$

Then the Bernstein inequality

$$\mathbb{P}\biggl\{\sup_{0\leqslant s\leqslant t}\Bigl|\tilde{\sigma}_1\int_{t_0}^t \mathrm{d}W_s^{(1)}\Bigr| \geqslant h_1\biggr\} \leqslant 2\exp\biggl\{-\frac{h_1^2}{2(t-t_0)\tilde{\sigma}_1^2}\biggr\} \tag{A.19}$$

yields (A.9). □

A.2 The nonlinear equation

We now turn to the analysis of the full system (4.6), or, equivalently, (A.2). Before that, we state a generalised Bernstein inequality that we will need several times in the sequel. Let W_t be an n-dimensional standard Brownian motion, and consider the martingale

$$M_t = \int_{t_0}^t g(X_s,s)\;\mathrm{d}W_s = \sum_{i=1}^n \int_{t_0}^t g_i(X_t,t)\;\mathrm{d}W_t^{(i)}\;, \tag{A.20}$$

where $g = (g_1,\dots,g_n)$ takes values in $\mathbb{R}^n$ and the process X_t is assumed to be adapted to the filtration generated by W_t. Then we have the following result (for the proof, see [BGK10, Lemma D.8]):

Lemma A.2. *Assume that the integrand satisfies*

$$g(X_t,t)g(X_t,t)^T \leqslant G(t)^2 \tag{A.21}$$

almost surely, for a deterministic function $G(t)$, and that the integral

$$V(t) = \int_{t_0}^t G(s)^2\;\mathrm{d}s \tag{A.22}$$

is finite. Then

$$\mathbb{P}\biggl\{\sup_{t_0\leqslant s\leqslant t} M_s > x\biggr\} \leqslant \mathrm{e}^{-x^2/2V(t)} \tag{A.23}$$

for any $x > 0$.

Proposition A.3. *Assume* $z_0 = \mathcal{O}(\tilde{\mu}^{1-\gamma})$. *There exist constants* $C, \kappa, M > 0$ *such that for* $t_0 \leqslant t \leqslant T + \mathcal{O}(|\log\tilde{\mu}|^{-1/2})$, *all* $\tilde{\sigma} \leqslant \tilde{\mu}$ *and* $H > 0$,

$$\mathbb{P}\biggl\{\sup_{t_0\leqslant s\leqslant t} \frac{|z_s - z_s^0|}{\sqrt{\zeta(s)}} \geqslant H\biggr\} \leqslant \frac{CT}{\tilde{\mu}^{2\gamma}}\biggl(\exp\biggl\{-\kappa\frac{\bigl[H - M(T^2\tilde{\mu}^{2-4\gamma} + T\tilde{\varepsilon}\tilde{\mu}^{-2\gamma})\bigr]^2}{\tilde{\sigma}^2}\biggr\} + \mathrm{e}^{-\kappa\tilde{\mu}^2/\tilde{\sigma}^2}\biggr) \tag{A.24}$$

and for all $H' > 0$,

$$\mathbb{P}\biggl\{\sup_{t_0\leqslant s\leqslant t} |u_s - u_s^0| \geqslant H'\biggr\} \leqslant \frac{CT}{\tilde{\mu}^{2\gamma}}\biggl(\exp\biggl\{-\kappa\frac{\bigl[H' - M(T^2\tilde{\mu}^{2-4\gamma} + T\tilde{\varepsilon}\tilde{\mu}^{-2\gamma})\bigr]^2}{\tilde{\sigma}^2\tilde{\mu}^{-2\gamma}}\biggr\} + \mathrm{e}^{-\kappa\tilde{\mu}^2/\tilde{\sigma}^2}\biggr)\,. \tag{A.25}$$

Proof: The upper bound on t implies that $\mathrm{e}^{t^2/2} = \mathcal{O}(\tilde{\mu}^{-\gamma})$. Thus it follows from (A.3) and (A.4) that

$$z_s^0 = \mathcal{O}(\tilde{\mu}^{1-\gamma}) \qquad \text{and} \qquad u_s^0 = \mathcal{O}(T\tilde{\mu}^{1-\gamma}) \tag{A.26}$$

for $t_0 \leqslant s \leqslant t$. Given $h, h_1, h_2 > 0$, we introduce the stopping times

$$\begin{aligned}\tau_1 &= \inf\Bigl\{s \geqslant t_0 \colon |z_s^1 - z_s^0| \geqslant h\sqrt{\zeta(s)}\Bigr\}\,,\\ \tau_2 &= \inf\biggl\{s \geqslant t_0 \colon |u_s^1 - u_s^0| \geqslant h_1 + h_2\int_{t_0}^t \sqrt{\zeta(s)}\,\mathrm{d}s\biggr\}\,.\end{aligned} \tag{A.27}$$

The integral of $\sqrt{\zeta(s)}$ is of order $T\tilde{\mu}^{-\gamma}$ at most. Thus choosing $h = h_1 = h_2 = \tilde{\mu}$ guarantees that

$$z_s^1 = \mathcal{O}(\tilde{\mu}^{1-\gamma}) \qquad \text{and} \qquad u_s^1 = \mathcal{O}(T\tilde{\mu}^{1-\gamma}) \tag{A.28}$$

for $t_0 \leqslant s \leqslant t \wedge \tau_1 \wedge \tau_2$. For these values of h, h_1 and h_2, Proposition A.1 implies that

$$\begin{aligned}\mathbb{P}\bigl\{\tau_1 < t\bigr\} &\leqslant cT\tilde{\mu}^{-2\gamma}\,\mathrm{e}^{-\kappa\tilde{\mu}^2/\tilde{\sigma}^2}\,,\\ \mathbb{P}\bigl\{\tau_2 < t\bigr\} &\leqslant cT\tilde{\mu}^{-2\gamma}\,\mathrm{e}^{-\kappa\tilde{\mu}^2/\tilde{\sigma}^2}\end{aligned} \tag{A.29}$$

for some constants $\kappa, c > 0$. We consider the difference $(x_t^2, y_t^2) = (u_t, z_t) - (u_t^1, z_t^1)$, which satisfies the system of SDEs

$$\begin{aligned}\mathrm{d}x_t^2 &= \bigl(-y_t^2 + \mathcal{O}(\tilde{\varepsilon})\bigr)\,\mathrm{d}t\,,\\ \mathrm{d}y_t^2 &= \bigl[ty_t^2 + 2(u_t^1 + x_t^2)(z_t^1 + y_t^2) + \mathcal{O}(\tilde{\varepsilon})\bigr]\,\mathrm{d}t - 2\tilde{\sigma}_1(u_t^1 + x_t^2)\,\mathrm{d}W_t^{(1)}\,.\end{aligned} \tag{A.30}$$

We introduce a Lyapunov function $U_t > 0$ defined by

$$(U_t - C_0)^2 = \frac{\bigl(x_t^2\bigr)^2 + \bigl(y_t^2\bigr)^2}{2}\,. \tag{A.31}$$

The constant C_0 will be chosen in order to kill the second-order terms arising from Itô's formula. Let

$$\tau^* = \inf\{t \geqslant t_0 \colon U_t = 1\}\,. \tag{A.32}$$

Applying Itô's formula and choosing C_0 of order $\tilde{\sigma}_1^2 \tilde{\mu}^{-(1-\gamma)}$ yields

$$\mathrm{d}U_t \leqslant \big[C_1 + C_2(t)U_t\big]\,\mathrm{d}t + \tilde{\sigma}_1 g(t)\,\mathrm{d}W_t^1 \;, \tag{A.33}$$

where (using the fact that $\tilde{\sigma} \leqslant \tilde{\mu}$)

$$\begin{aligned} C_1 &= \mathcal{O}\big(T\tilde{\mu}^{2-2\gamma}\big) + \mathcal{O}(\tilde{\varepsilon}) \;, \\ C_2(t) &= t \vee 0 + \mathcal{O}(T\tilde{\mu}^{1-\gamma}) \;, \end{aligned} \tag{A.34}$$

and $g(t)$ is at most of order 1 for $t \leqslant \tau_1 \wedge \tau_2 \wedge \tau^*$. Hence

$$U_{t\wedge\tau_1\wedge\tau_2\wedge\tau^*} \leqslant U_{t_0} + C_1(t-t_0) + \int_{t_0}^{t\wedge\tau_1\wedge\tau_2\wedge\tau^*} C_2(s)U_s\,\mathrm{d}s + \tilde{\sigma}_1 \int_{t_0}^{t\wedge\tau_1\wedge\tau_2\wedge\tau^*} g(s)\,\mathrm{d}W_s^1 \;. \tag{A.35}$$

We introduce a last stopping time

$$\tau_3 = \inf\biggl\{ t \geqslant t_0 \colon \biggl| \tilde{\sigma}_1 \int_0^{t\wedge\tau_1\wedge\tau_2\wedge\tau^*} g(s)\,\mathrm{d}W_s^1 \biggr| \geqslant h_3 \biggr\} \;. \tag{A.36}$$

Then Lemma A.2 implies

$$\mathbb{P}\big\{\tau_3 < t\big\} \leqslant \mathrm{e}^{-\kappa_3 h_3^2/\tilde{\sigma}_1^2} \tag{A.37}$$

for a $\kappa_3 > 0$. Applying Gronwall's lemma to (A.35) we get

$$\begin{aligned} U_{t\wedge\tau_1\wedge\tau_2\wedge\tau_3\wedge\tau^*} &\leqslant \big[U_{t_0} + C_1(t-t_0) + h_3\big] \exp\biggl\{ \int_{t_0}^{t\wedge\tau_1\wedge\tau_2\wedge\tau_3\wedge\tau^*} C_2(u)\,\mathrm{d}u \biggr\} \\ &= \mathcal{O}(T^2\tilde{\mu}^{2-3\gamma}) + \mathcal{O}(\tilde{\sigma}^2 T^2 \tilde{\mu}^{1-2\gamma}) + \mathcal{O}(\tilde{\varepsilon} T \tilde{\mu}^{-\gamma}) \;. \end{aligned} \tag{A.38}$$

This shows in particular that $\tau^* > t$, provided we take γ small enough. Now (A.24) follows from the decomposition

$$\begin{aligned} \mathbb{P}\biggl\{ \sup_{t_0\leqslant s\leqslant t} \frac{|z_s - z_s^0|}{\sqrt{\zeta(s)}} \geqslant H \biggr\} &\leqslant \mathbb{P}\biggl\{ \sup_{t_0\leqslant s\leqslant t\wedge\tau_1\wedge\tau_2\wedge\tau_3} \frac{|z_s^1 - z_s^0|}{\sqrt{\zeta(s)}} \geqslant H - \sup_{t_0\leqslant s\leqslant t\wedge\tau_1\wedge\tau_2\wedge\tau_3} \frac{U_s}{\sqrt{\zeta(s)}} \biggr\} \\ &\quad + \mathbb{P}\big\{\tau_1 > t\big\} + \mathbb{P}\big\{\tau_2 > t\big\} + \mathbb{P}\big\{\tau_3 > t\big\} \;, \end{aligned} \tag{A.39}$$

and (A.25) is obtained in a similar way. □

We can now derive bounds for the contribution of the motion near the separatrix to the Markov kernel.

Proposition A.4. *Fix some $\gamma \in (0, 1/4)$ and an initial condition $(\xi_0, z_0) = (-L, z_0) \in F_-$ with $|z_0| = \mathcal{O}(\tilde{\mu}^{1-\gamma})$.*

1. *Assume $c = 0$. Then there exist constants $C, \kappa_1, h_0 > 0$ such that the sample path starting in (ξ_0, z_0) will hit F_+ for the first time at a point (ξ_1, z_1) such that*

$$\mathbb{P}\biggl\{ z_1 \leqslant z_T^0 - \tilde{\mu} \biggr\} \leqslant \frac{C}{\tilde{\mu}^{2\gamma}} \exp\biggl\{ -\kappa_1 \frac{\tilde{\mu}^2}{\tilde{\sigma}^2} \biggr\} \;. \tag{A.40}$$

2. *If $c \neq 0$, but $\sqrt{\varepsilon} \leqslant \tilde{\mu}^{1+2\gamma+\theta}$ for some $\theta > 0$, then the first-hitting point of F_+ always satisfies*

$$\mathbb{P}\biggl\{ |z_1 - z_T^0| \geqslant \tilde{\mu} \biggr\} \leqslant \frac{C}{\tilde{\mu}^{2\gamma}} \exp\biggl\{ -\kappa_1 \frac{\tilde{\mu}^2}{\tilde{\sigma}^2} \biggr\} \;. \tag{A.41}$$

PROOF: Consider first the case $\sqrt{\varepsilon} \leqslant \tilde{\mu}^{1+2\gamma+\theta}$. For any $h > 0$ we can write

$$\mathbb{P}\big\{|z_\tau - z_T^0| \geqslant \tilde{\mu}\big\} \leqslant \mathbb{P}\big\{|z_\tau - z_\tau^0| \geqslant \tilde{\mu} - h\tilde{\mu}^{2-2\gamma}\big\} + \mathbb{P}\big\{|z_\tau^0 - z_T^0| \geqslant h\tilde{\mu}^{2-2\gamma}\big\} \,. \tag{A.42}$$

The first term on the right-hand side can be bounded, using (A.24), by a term of order $\tilde{\mu}^{-2\gamma}\,\mathrm{e}^{-\kappa_1\tilde{\mu}^2/\tilde{\sigma}^2}$. The conditions on γ and $\sqrt{\varepsilon}$ ensure that the error terms in the exponent in (A.24) are negligible.

To bound the second term on the right-hand side, we note that (A.3) implies that $|z_\tau^0 - z_T^0|$ has order $\tilde{\mu}^{1-\gamma}|\tau - T|$. Furthermore, the definitions of τ and u^0 imply that $|\tau - T| = 2|u_t - u_t^0| + \mathcal{O}(\tilde{\mu}^{1-\gamma})$. This shows that

$$\mathbb{P}\big\{|z_\tau^0 - z_T^0| \geqslant h\tilde{\mu}^{2-2\gamma}\big\} \leqslant \mathbb{P}\big\{|u_t - u_t^0| \geqslant hc_1\tilde{\mu}^{1-\gamma} - c_2\mu^{1-\gamma}\big\} \tag{A.43}$$

for some constants $c_1, c_2 > 0$. Taking $h = 2c_2/c_1$ and using (A.25) yields a similar bound as for the first term.

In the case $c = 0$, we can conclude in the same way by observing that z_t is bounded below by its value for $\varepsilon = 0$, the ε-dependent term of $\mathrm{d}z_t$ in (4.6) being positive. Thus we need no condition on $\sqrt{\varepsilon}$ for the error terms in the exponent to be negligible. □

B Dynamics during an SAO

B.1 Action–angle-type variables

In this section, we construct another set of coordinates allowing to describe the dynamics during a small-amplitude oscillation. In the limit $\varepsilon \to 0$ and $\tilde{\mu} \to 0$, the deterministic system (4.4) becomes

$$\begin{aligned} \dot{\xi} &= \frac{1}{2} - z \\ \dot{z} &= 2\xi z \,. \end{aligned} \tag{B.1}$$

This system admits a first integral

$$Q = 2z\,\mathrm{e}^{-2z-2\xi^2+1} \,, \tag{B.2}$$

which is equivalent to the first integral found in [BE92]. The normalisation is chosen in such a way that $Q \in [0,1]$ for $z \geqslant 0$. The separatrix is given in this limit by $Q = 0$, while $Q = 1$ corresponds to the stationary point P. When ε and $\tilde{\mu}$ are positive, we obtain

$$\dot{Q} = \left[2\tilde{\mu}(1-2z) + \sqrt{\varepsilon}\left(\frac{4}{9\alpha_*^2}\xi^4 + c\big[4z\xi^2 - 6\xi^2 + 8z^2 - 4z + 1\big]\right)\right]\mathrm{e}^{-2z-2\xi^2+1} \,. \tag{B.3}$$

Observe that if $c = 0$, the term of order $\sqrt{\varepsilon}$ is strictly positive.

In order to analyse the dynamics in more detail, it is useful to introduce an angle variable ϕ. We define a coordinate transformation from $(0,1] \times \mathbb{S}^1$ to $\mathbb{R} \times \mathbb{R}_+$ by

$$\begin{aligned} \xi &= -\sqrt{\frac{-\log Q}{2}}\,\sin\phi \\ z &= \frac{1}{2}\left(1 + f\left(\sqrt{\frac{-\log Q}{2}}\,\cos\phi\right)\right) \,. \end{aligned} \tag{B.4}$$

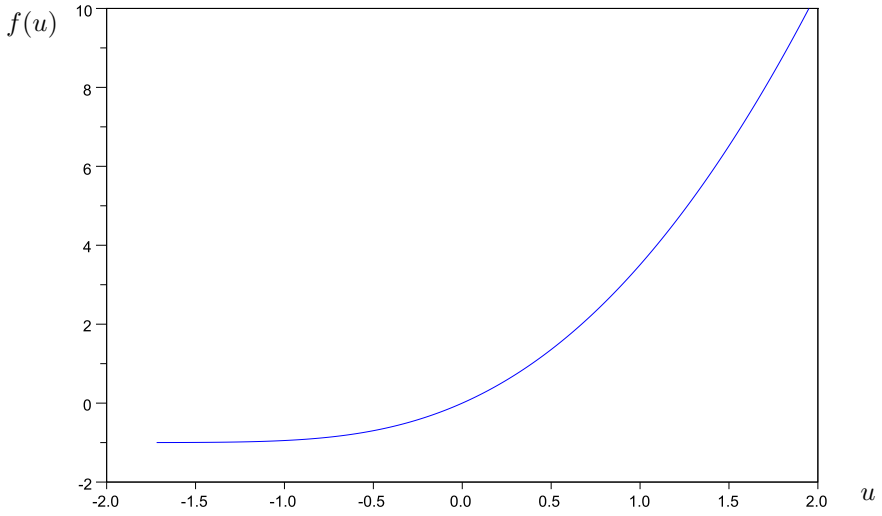

FIGURE 9. Graph of $u \mapsto f(u)$.

Here $f : \mathbb{R} \to (-1, +\infty)$ is defined as the solution of

$$\log(1 + f(u)) - f(u) = -2u^2 \tag{B.5}$$

such that

$$\operatorname{sign} f(u) = \operatorname{sign} u \ . \tag{B.6}$$

The graph of f is plotted in Figure 9.

Lemma B.1. *The function f has the following properties:*

- *Lower bounds:*
$$f(u) > -1 \qquad \textit{and} \qquad f(u) \geqslant 2u \qquad \forall u \in \mathbb{R} \ . \tag{B.7}$$
- *Upper bounds: There exist constants $C_1, C_2 > 0$ and a function $r : \mathbb{R}_- \to \mathbb{R}$, with $0 \leqslant r(u) \leqslant C_1 \, \mathrm{e}^{-1-2u^2}$, such that*
$$f(u) \leqslant C_2 u + 2u^2 \qquad \forall u \geqslant 0 \ , \tag{B.8}$$
$$f(u) = -1 + \mathrm{e}^{-1-2u^2}[1 + r(u)] \qquad \forall u \leqslant 0 \ . \tag{B.9}$$
- *Derivatives: $f \in \mathcal{C}^\infty$ and*
$$f'(u) = 4u \frac{1 + f(u)}{f(u)} \ , \tag{B.10}$$
$$f''(u) = 4 \frac{1 + f(u)}{f(u)} \left(1 - 4 \frac{u^2}{f(u)^2} \right) \ . \tag{B.11}$$
- *There exists a constant $M > 0$ such that*
$$0 < f''(u) \leqslant M \quad \forall u \in \mathbb{R} \ . \tag{B.12}$$

PROOF: The results follow directly from the implicit function theorem and elementary calculus. □

We can now derive an expression for the SDE in coordinates (Q, ϕ). To ease notation, we introduce the function

$$X = X(Q, \phi) = \sqrt{\frac{-\log Q}{2}} \cos \phi \,, \tag{B.13}$$

a parameter $\tilde{\sigma} > 0$ defined by

$$\tilde{\sigma}^2 = \tilde{\sigma}_1^2 + \tilde{\sigma}_2^2 \,, \tag{B.14}$$

and the two-dimensional Brownian motion $\mathrm{d}W_t = (\mathrm{d}\tilde{W}_t^{(1)}, \mathrm{d}\tilde{W}_t^{(2)})^T$.

Proposition B.2. *For $z > 0$, the system of SDEs (4.6) is equivalent to the system*

$$\begin{aligned} \mathrm{d}Q_t &= \tilde{\mu} f_1(Q_t, \phi_t)\ \mathrm{d}t + \tilde{\sigma} \psi_1(Q_t, \phi_t)\, \mathrm{d}W_t \\ \mathrm{d}\phi_t &= f_2(Q_t, \phi_t)\ \mathrm{d}t + \tilde{\sigma} \psi_2(Q_t, \phi_t)\, \mathrm{d}W_t \,, \end{aligned} \tag{B.15}$$

where we introduced the following notations.

- *The new drift terms are of the form*

$$f_1(Q, \phi) = -2Q \frac{f(X)}{1 + f(X)} \left[1 + \frac{\sqrt{\varepsilon}}{\tilde{\mu}} R_{Q,\varepsilon}(Q, \phi) + \frac{\tilde{\sigma}^2}{\tilde{\mu}} R_{Q,\sigma}(Q, \phi) \right] , \tag{B.16}$$

$$f_2(Q, \phi) = \frac{f(X)}{2X} \left[1 + \frac{2\tilde{\mu} \tan \phi}{\log Q (1 + f(X))} + \sqrt{\varepsilon} R_{\phi,\varepsilon}(Q, \phi) + \tilde{\sigma}^2 R_{\phi,\sigma}(Q, \phi) \right] . \tag{B.17}$$

- *The remainders in the drift terms are bounded as follows. Let*

$$\rho(Q, \phi) = \begin{cases} \sqrt{|\log Q|} & \text{if } \cos \phi \geqslant 0 \,, \\ Q^{-\cos^2 \phi} & \text{if } \cos \phi < 0 \,. \end{cases} \tag{B.18}$$

  Then there exists a constant $M_1 > 0$ such that for all $Q \in (0, 1)$ and all $\phi \in \mathbb{S}^1$,

$$\begin{aligned} &|R_{Q,\varepsilon}(Q, \phi)| \leqslant M_1 |\log Q|^2 \,, && |R_{Q,\sigma}(Q, \phi)| \leqslant M_1 \rho(Q, \phi) \,, \\ &|R_{\phi,\varepsilon}(Q, \phi)| \leqslant M_1 |\log Q|^{3/2} \rho(Q, \phi) \,, && |R_{\phi,\sigma}(Q, \phi)| \leqslant M_1 \rho(Q, \phi)^2 / |\log Q| \,. \end{aligned} \tag{B.19}$$

  Furthermore, if $c = 0$ then $-f(X) R_{Q,\varepsilon}(Q, \phi) \geqslant 0$.
- *The diffusion coefficients are given by*

$$\begin{aligned} \psi_1(Q, \phi) &= \left(2\sqrt{2} \frac{\tilde{\sigma}_1}{\tilde{\sigma}} Q \left[\sqrt{-\log Q} - \frac{f(X)}{1 + f(X)} \right] \sin \phi, -2 \frac{\tilde{\sigma}_2}{\tilde{\sigma}} Q \frac{f(X)}{1 + f(X)} \right) , \\ \psi_2(Q, \phi) &= \left(-\frac{\tilde{\sigma}_1}{\tilde{\sigma}} \sqrt{\frac{2}{-\log Q}} \frac{1 + f(X) \cos \phi}{[1 + f(X)] \cos \phi}, \frac{\tilde{\sigma}_2}{\tilde{\sigma}} \frac{1}{\log Q} \frac{f(X)}{1 + f(X)} \tan \phi \right) . \end{aligned} \tag{B.20}$$

- *There exists a constant $M_2 > 0$ such that for all $Q \in (0, 1)$ and all $\phi \in \mathbb{S}^1$,*

$$\|\psi_1(Q, \phi)\|^2 \leqslant M_2 Q^2 \rho(Q, \phi)^2 \,, \qquad \|\psi_2(Q, \phi)\|^2 \leqslant M_2 \frac{\rho(Q, \phi)^2}{|\log Q|^2} \,. \tag{B.21}$$

Proof: The result follows from Itô's formula, by a straightforward though lengthy computation. The difference between the bounds obtained for $\cos \phi \geqslant 0$ and $\cos \phi < 0$ is due to the fact that terms such as $f(X) \tan(\phi)/(1 + f(X))$ can be bounded by a constant times $\sqrt{-\log Q}$ in the first case, and by a constant times $Q^{-\cos^2 \phi}$ in the second one, as a consequence of Lemma B.1. The fact that $-f(X) R_{Q,\varepsilon}$ is positive if $c = 0$ follows from the positivity of the term of order $\sqrt{\varepsilon}$ in (B.3). □

B.2 Averaging

In System (B.15), the variable Q changes more slowly than the variable ϕ, which is a consequence of the fact that Q is a first integral when $\tilde{\mu} = \varepsilon = \tilde{\sigma} = 0$. This suggests to use an averaging approach to analyse the dynamics. However, since the behaviour near $\phi = \pi$ has already been considered in the previous section, using (ξ, z)-coordinates, we only need to consider $\phi \in [\phi_0, \phi_1]$, where $-\pi < \phi_0 < 0 < \phi_1 < \pi$.

We look for a change of variables of the form

$$\overline{Q} = Q + \tilde{\mu} w(Q, \phi) \tag{B.22}$$

which eliminates the term of order $\tilde{\mu}$ in $\mathrm{d}Q_t$. Itô's formula yields

$$\mathrm{d}\overline{Q}_t = \mathrm{d}Q_t + \tilde{\mu}\frac{\partial w}{\partial \phi}\,\mathrm{d}\phi_t + \tilde{\mu}\frac{\partial w}{\partial Q}\,\mathrm{d}Q_t + \frac{1}{2}\tilde{\mu}\left(\frac{\partial^2 w}{\partial Q^2}\,\mathrm{d}Q_t^2 + 2\frac{\partial^2 w}{\partial Q\,\partial \phi}\,\mathrm{d}Q_t\,d\phi_t + \frac{\partial^2 w}{\partial \phi^2}\,\mathrm{d}\phi_t^2\right). \tag{B.23}$$

Replacing dQ_t et $d\phi_t$ by their expressions in (B.15), we get

$$\mathrm{d}\overline{Q}_t = \tilde{\mu}\left(f_1 + \frac{\partial w}{\partial \phi} f_2 + \mathcal{O}(\tilde{\mu}) + \mathcal{O}(\tilde{\sigma}^2)\right)\mathrm{d}t + \tilde{\sigma}\left(\psi_1 + \tilde{\mu}\left(\frac{\partial w}{\partial \phi}\psi_2 + \frac{\partial w}{\partial Q}\psi_1\right)\right)\mathrm{d}W_t\,. \tag{B.24}$$

Thus choosing the function w in such a way that

$$f_1 + \frac{\partial w}{\partial \phi} f_2 = 0 \tag{B.25}$$

will decrease the order of the drift term in (B.24). We thus define the function w by the integral

$$w(Q, \phi) = -\int_{\phi_0}^{\phi} \frac{f_1(Q, \theta)}{f_2(Q, \theta)}\,\mathrm{d}\theta\,, \tag{B.26}$$

which is well-defined (i.e., there are no resonances), since (B.7) shows that $f_2(Q, \phi)$ is bounded below by a positive constant, for sufficiently small $\tilde{\mu}$, ε and $\tilde{\sigma}$.

Lemma B.3. *Let $\phi_0 \in (-\pi, -\pi/2)$ and $\phi_1 \in (\pi/2, \pi)$ be such that $\cos^2(\phi_0), \cos^2(\phi_1) \leqslant b$ for some $b \in (0, 1)$. Then*

$$w(Q, \phi_1) = -\frac{\sqrt{2}\,\mathrm{e}}{\sqrt{-\log Q}}\left[\frac{Q^{\sin^2\phi_0}}{-\sin\phi_0} + \frac{Q^{\sin^2\phi_1}}{\sin\phi_1} + r_1(Q)\right]\Big(1 + r_2(Q) + r_\varepsilon(Q)\Big)\,, \tag{B.27}$$

where the remainder terms satisfy

$$\begin{aligned}
r_1(Q) &= \mathcal{O}\big(Q\log(|\log Q|)\big)\,,\\
r_2(Q) &= \mathcal{O}\left(\frac{1}{|\log Q|} + \tilde{\mu}Q^{-b} + \tilde{\sigma}^2\left(\frac{Q^{-b}}{\tilde{\mu}} + \frac{Q^{-2b}}{|\log Q|}\right)\right),\\
r_\varepsilon(Q) &\leqslant \sqrt{\varepsilon}\,\mathcal{O}\left(\frac{|\log Q|^2}{\tilde{\mu}} + Q^{-b}|\log Q|^{3/2}\right),
\end{aligned} \tag{B.28}$$

and $r_\varepsilon(Q) \geqslant 0$ is $c = 0$. Furthermore, the derivatives of w satisfy the bounds

$$\frac{\partial w}{\partial Q}(Q, \phi) = \mathcal{O}\left(\frac{Q^{-b}}{\sqrt{|\log Q|}}\right), \qquad \frac{\partial w}{\partial \phi}(Q, \phi) = \mathcal{O}\big(Q^{1-b}\sqrt{|\log Q|}\big)\,, \tag{B.29}$$

and

$$\frac{\partial^2 w}{\partial Q^2} = \mathcal{O}\Big(\frac{Q^{-1-b}}{\sqrt{|\log Q|}}\Big)\,, \quad \frac{\partial^2 w}{\partial Q \partial \phi} = \mathcal{O}\Big(\frac{Q^{-b}}{\sqrt{|\log K|}}\Big)\,, \quad \frac{\partial^2 w}{\partial \phi^2} = \mathcal{O}(Q^{1-b}\sqrt{|\log Q|})\,. \tag{B.30}$$

PROOF: We split the integral into three parts. Using the change of variables $t = \sin\phi$ and a partial fraction decomposition, we find that the leading part of the integral on $[-\pi/2, \pi/2]$ satisfies

$$\int_{-\pi/2}^{\pi/2} \frac{4QX(Q,\phi)}{1+f(X(Q,\phi))}\,\mathrm{d}\phi = \mathcal{O}\Big(Q\frac{\log(|\log Q|)}{\sqrt{|\log Q|}}\Big)\,. \tag{B.31}$$

Next we consider the integral on $[\phi_0, -\pi/2]$. The change of variables $u = \sqrt{-2\log Q}\sin\phi$, (B.9) and asymptotic properties of the error function imply

$$\begin{aligned}\int_{\phi_0}^{-\pi/2} \frac{4QX}{1+f(X)}\,\mathrm{d}\phi &= 2Q\int_{\sin\phi_0\sqrt{-2\log Q}}^{-\sqrt{-2\log Q}} \frac{\mathrm{d}u}{1+f\Big(-\sqrt{\frac{-\log Q}{2}-\frac{u^2}{4}}\Big)} \\ &= 2\,\mathrm{e}\int_{\sin\phi_0\sqrt{-2\log Q}}^{-\sqrt{-2\log Q}} \mathrm{e}^{-u^2/2}\big[1+\mathcal{O}(Q\,\mathrm{e}^{-u^2/2})\big]\,\mathrm{d}u \\ &= -2\,\mathrm{e}\,\frac{Q^{\sin^2\phi_0}}{\sqrt{-2\log Q}(-\sin\phi_0)}\Big[1+\mathcal{O}\Big(\frac{1}{|\log Q|}\Big)+\mathcal{O}(Q^{\cos^2\phi_0})\Big]\,.\end{aligned} \tag{B.32}$$

The integral on $[\pi/2, \phi_1]$ can be computed in a similar way. This yields the leading term in (B.27), and the form of the remainders follows from (B.19) with $\rho = Q^{-b}$. The bound on $\partial w/\partial\phi$ follows directly from (B.25), while the bound on $\partial w/\partial Q$ is obtained by computing the derivative of f_1/f_2. The bounds on second derivatives follow by similar computations. □

Notice that for the remainder $r_2(Q)$ to be small, we need that $Q^b \gg \tilde{\mu}$ and $Q^b \gg \tilde{\sigma}^2/\tilde{\mu}$. Then the term $r_\varepsilon(Q)$ is of order $\sqrt{\varepsilon}|\log\tilde{\mu}|^2/\tilde{\mu}$, which is small for $\tilde{\mu}/|\log\tilde{\mu}|^2 \gg \sqrt{\varepsilon}$. If that is the case, then $w(Q,\phi_1)$ has order $Q^{1-b}/\sqrt{|\log Q|}$. Otherwise, $w(Q,\phi_1)$ has order $\sqrt{\varepsilon}Q^{1-b}|\log Q|^{3/2}/\tilde{\mu}$. In the sequel, we will sometimes bound $1/\sqrt{|\log Q|}$ by 1 to get simpler expressions.

B.3 Computation of the kernel

We can now proceed to the computation of the rotational part of the kernel of the Markov chain. Recall the broken lines $F_\pm$ introduced in (4.18) and (4.19). For an initial condition $(L, z_0) \in F_+$, we want to compute the coordinates of the point (ξ_τ, z_τ) at the first time

$$\tau = \inf\big\{t > 0\colon (\xi_t, z_t) \in F_-\big\} \tag{B.33}$$

that the path starting in (L, z_0) hits F_-.

We will assume that there is a $\beta \in (0,1]$ such that

$$(c_-\tilde{\mu})^\beta \leqslant z_0 \leqslant z_{\max} < \frac{1}{2}\,. \tag{B.34}$$

The (Q,ϕ)-coordinates of the initial condition are given by

$$Q_0 = 2z_0\,\mathrm{e}^{1-2z_0}\,\mathrm{e}^{-2L^2} \geqslant 2(c_-\tilde\mu)^{\beta+\gamma}\;,$$
$$\sin^2\phi_0 = \frac{2L^2}{-\log Q_0} \geqslant \frac{\gamma}{\beta+\gamma}\;, \tag{B.35}$$

with $\phi_0 \in (-\pi,-\pi/2)$. Thus Lemma B.3 applies with $b=\beta/(\beta+\gamma)<1$. Notice that

$$Q_0^{\cos^2\phi_0} \geqslant 2^b(c_-\tilde\mu)^\beta\;. \tag{B.36}$$

Proposition B.4. *Assume z_0 satisfies* (B.34) *for a $\beta<1$. Then there exists a constant $\kappa>0$ such that the following holds for sufficiently small $\tilde\mu$ and $\tilde\sigma$.*

1. *If $\sqrt{\varepsilon}\leqslant\tilde\mu/|\log\tilde\mu|^2$, then with probability greater or equal than*

$$1-\mathrm{e}^{-\kappa\tilde\mu^2/\tilde\sigma^2}\;, \tag{B.37}$$

(ξ_t,z_t) hits F_- for the first time at a point $(-L,z_1)$ such that

$$z_1 = z_0+\tilde\mu A(z_0)+\frac{z_0}{1-2z_0}\Big[\tilde\sigma V(z_0)+\mathcal{O}\big(\tilde\mu^{2(1-\beta)}+\tilde\sigma^2\tilde\mu^{-2\beta}\big)\Big]\;. \tag{B.38}$$

The function $A(z_0)$ is given by

$$A(z_0)=\frac{\mathrm{e}^{2z_0}}{L(1-2z_0)}\left[1+\mathcal{O}\big(z_0\log|\log\tilde\mu|\big)+\mathcal{O}\left(\frac{1}{|\log z_0|}\right)\right]\;, \tag{B.39}$$

and $V(z_0)$ is a random variable satisfying

$$\mathbb{P}\big\{\tilde\sigma|V(z_0)|\geqslant h\big\}\leqslant 2\exp\left\{-\frac{\kappa h^2\tilde\mu^{2\beta}}{\tilde\sigma^2}\right\}\qquad\forall h>0\;. \tag{B.40}$$

2. *If $c=0$ and $\sqrt{\varepsilon}>\tilde\mu/|\log\tilde\mu|^2$, then (ξ_t,z_t) hits F_- for the first time either at a point $(-L,z_1)$ such that z_1 is greater or equal than the right-hand side of* (B.38)*, or at a point $(\xi_1,1/2)$ with $-L\leqslant\xi_1\leqslant 0$, again with a probability bounded below by* (B.37)*.*

Proof: We first consider the case $\sqrt{\varepsilon}\leqslant\tilde\mu/|\log\tilde\mu|^2$.

- **Step 1 :** To be able to bound various error terms, we need to assume that Q_t stays bounded below. We thus introduce a second stopping time

$$\tau_1=\inf\big\{t>0\colon\ \cos\phi_t<0, Q_t^{\cos^2\phi_t}<(c_-\tilde\mu)^\beta\big\}\;. \tag{B.41}$$

We start by showing that $\tau\wedge\tau_1$ is bounded with high probability. Proposition B.2 implies the existence of a constant $C>0$ such that

$$\mathrm{d}\phi_t \geqslant C\,\mathrm{d}t+\tilde\sigma\psi_2(Q_t,\phi_t)\,\mathrm{d}W_t\;. \tag{B.42}$$

Integrating this relation between 0 and t, we get

$$\phi_t\geqslant\phi_0+Ct+\tilde\sigma\int_0^t\psi_2(Q_s,\phi_s)\,\mathrm{d}W_s\;. \tag{B.43}$$

Lemma A.2 and (B.21) provide the bound

$$\mathbb{P}\left\{\left|\tilde\sigma\int_0^{t\wedge\tau_1}\psi_2(Q_s,\phi_s)\,\mathrm{d}W_s\right|\geqslant h\right\}\leqslant\exp\left\{-\frac{\kappa h^2\tilde\mu^{2\beta}}{\tilde\sigma^2}\right\} \tag{B.44}$$

for some $\kappa > 0$. Since by definition, $\phi_{\tau\wedge\tau_1} - \phi_0 < 2\pi$, we get

$$\mathbb{P}\Big\{\tau \wedge \tau_1 > \frac{2\pi + h}{C}\Big\} \leqslant \exp\Big\{-\frac{\kappa h^2 \tilde{\mu}^{2\beta}}{\tilde{\sigma}^2}\Big\} . \tag{B.45}$$

From now on, we work on the set $\Omega_1 = \{\tau \wedge \tau_1 \leqslant (2\pi + 1)/C\}$, which has probability greater or equal $1 - \mathrm{e}^{-\kappa\tilde{\mu}^{2\beta}/\tilde{\sigma}^2}$.

- **Step 2 :** The SDE (B.23) for $\overline{Q}_t$ can be written

$$\mathrm{d}\overline{Q}_t = \overline{Q}_t \bar{f}(\overline{Q}_t, \phi_t)\,\mathrm{d}t + \tilde{\sigma}\overline{Q}_t \bar{\psi}(\overline{Q}_t, \phi_t)\,\mathrm{d}W_t , \tag{B.46}$$

where the bounds in Proposition B.2 and Lemma B.3 yield

$$\begin{aligned} \bar{f}(\overline{Q}, \phi) &= \mathcal{O}\big(\tilde{\mu}^{2(1-\beta)} + \tilde{\sigma}^2\tilde{\mu}^{1-3\beta}\big) , \\ \|\bar{\psi}(\overline{Q}, \phi)\|^2 &= \mathcal{O}\big(\tilde{\mu}^{-2\beta}\big) . \end{aligned} \tag{B.47}$$

By Itô's formula, the variable $Z_t = \log \overline{Q}_t$ satisfies

$$\mathrm{d}Z_t = \tilde{f}(Z_t, \phi_t)\,\mathrm{d}t + \tilde{\sigma}\tilde{\psi}(Z_t, \phi_t)\,\mathrm{d}W_t , \tag{B.48}$$

where $\tilde{f}(Z, \phi) = \bar{f}(\mathrm{e}^Z, \phi) + \mathcal{O}(\tilde{\sigma}^2\tilde{\mu}^{-2\beta})$ and $\tilde{\psi}(Z, \phi) = \bar{\psi}(\mathrm{e}^Z, \phi)$. Setting

$$V_t = \int_0^t \tilde{\psi}(Z_s, \phi_s)\,\mathrm{d}W_s , \tag{B.49}$$

we obtain, integrating (B.48) and using the fact that $\tilde{\mu}^{1-3\beta} \leqslant \tilde{\mu}^{-2\beta}$,

$$Z_t = Z_0 + \tilde{\sigma}V + \mathcal{O}\big(\tilde{\mu}^{2(1-\beta)} + \tilde{\sigma}^2\tilde{\mu}^{-2\beta}\big) . \tag{B.50}$$

Another application of Lemma A.2 yields

$$\mathbb{P}\big\{\tilde{\sigma}|V_{t\wedge\tau_1}| \geqslant h_1\big\} \leqslant 2\exp\Big\{-\frac{\kappa_1 h_1^2 \tilde{\mu}^{2\beta}}{\tilde{\sigma}^2}\Big\} \tag{B.51}$$

for some $\kappa_1 > 0$. A convenient choice is $h_1 = \tilde{\mu}^{1-\beta}$. From now on, we work on the set $\Omega_1 \cap \Omega_2$, where $\Omega_2 = \{\tilde{\sigma}V_{t\wedge\tau_1} < \tilde{\mu}^{1-\beta}\}$ satisfies $\mathbb{P}(\Omega_2) \geqslant 1 - \mathrm{e}^{-\kappa_1\tilde{\mu}^2/\tilde{\sigma}^2}$.

- **Step 3 :** Returning to the variable $\overline{Q}$, we get

$$\overline{Q}_t = Q_0\,\mathrm{e}^{\tilde{\sigma}V_t}\Big[1 + \mathcal{O}\big(\tilde{\mu}^{2(1-\beta)} + \tilde{\sigma}^2\tilde{\mu}^{-2\beta}\big)\Big] , \tag{B.52}$$

and thus

$$Q_t = Q_0\,\mathrm{e}^{\tilde{\sigma}V_t}\Big[1 + \mathcal{O}\big(\tilde{\mu}^{2(1-\beta)} + \tilde{\sigma}^2\tilde{\mu}^{-2\beta}\big)\Big] - \tilde{\mu}w(Q_t, \phi_t) . \tag{B.53}$$

Using the implicit function theorem and the upper bound on w, we get the a priori bound

$$\frac{|Q_t - Q_0|}{Q_0} = \mathcal{O}\big(\tilde{\mu}^{1-\beta} + \tilde{\sigma}^2\tilde{\mu}^{-2\beta}\big) . \tag{B.54}$$

- **Step 4 :** The a priori estimate (B.54) implies that on $\Omega_1 \cap \Omega_2$, the sample path cannot hit F_- on the part $\{-L \leqslant \xi \leqslant 0, z = 1/2\}$. Indeed, this would imply that $Q_\tau \geqslant (c_-\tilde{\mu})^\gamma$, while $Q_0 \leqslant a(c_-\tilde{\mu})^\gamma$ with $a = 2z_{\max}\,\mathrm{e}^{1-2z_{\max}} < 1$. As a consequence, we would have $(Q_\tau - Q_0)/Q_0 > (1-a)/a$, contradicting (B.54).
  Let us now show that we also have $\tau_1 \geqslant \tau$ on $\Omega_1 \cap \Omega_2$. Assume by contradiction that $\tau_1 < \tau$. Then we have $Q_{\tau_1} = (c_-\tilde{\mu})^\beta$ and $\cos^2\phi_{\tau_1} < \beta/(\beta+\gamma)$, so that $Q_{\tau_1} = o(\tilde{\mu}^{\beta+\gamma})$. Thus $\tilde{\mu}w(Q_{\tau_1}, \phi_{\tau_1}) = \mathcal{O}(Q_{\tau_1}\tilde{\mu}^{1-\beta}) = o(\tilde{\mu}^{1+\gamma})$. Together with the lower bound (B.35) on Q_0, this implies that the right-hand side of (B.53) is larger than a constant times $\tilde{\mu}^{\beta+\gamma}$ at time $t = \tau_1$. But this contradicts the fact that $Q_{\tau_1} = o(\tilde{\mu}^{\beta+\gamma})$.

- **Step 5 :** The previous step implies that $\xi_\tau = -L$ on $\Omega_1 \cap \Omega_2$. We can thus write

$$\phi_\tau = g(Q_\tau) \qquad \text{where} \qquad \sin(g(Q)) = \sqrt{\frac{2}{-\log Q}}\, L \,, \tag{B.55}$$

with $g(Q) \in (\pi/2, \pi)$. Notice that $g(Q_0) = -\phi_0$. Furthermore, we have

$$g'(Q) = \frac{L}{\sqrt{2}Q(-\log Q)^{3/2}\cos(g(Q))} \,, \tag{B.56}$$

and thus $Q_\tau g'(Q_\tau) = \mathcal{O}(1/|\log\tilde{\mu}|)$. Using this in the Taylor expansion

$$w(Q_\tau, \phi_\tau) = w(Q_0, -\phi_0) + (Q_\tau - Q_0)\left[\frac{\partial w}{\partial Q}(Q_\theta, g(Q_\theta)) + \frac{\partial w}{\partial \phi}(Q_\theta, g(Q_\theta))g'(Q_\theta)\right] , \tag{B.57}$$

which holds for some $Q_\theta \in (Q_0, Q_\tau)$, yields the estimate

$$\frac{w(Q_\tau, \phi_\tau)}{Q_0} = \frac{w(Q_0, -\phi_0)}{Q_0} + \mathcal{O}\big(\tilde{\mu}^{1-2\beta} + \tilde{\sigma}^2\tilde{\mu}^{-3\beta}\big) \,. \tag{B.58}$$

Substitution in (B.53) yields the more precise estimate

$$Q_1 = Q_0\left[\mathrm{e}^{\tilde{\sigma}V_\tau} - \tilde{\mu}\frac{w(Q_0, -\phi_0)}{Q_0} + \mathcal{O}\big(\tilde{\mu}^{2(1-\beta)} + \tilde{\sigma}^2\tilde{\mu}^{1-3\beta}\big)\right] . \tag{B.59}$$

- **Step 6 :** Finally, we return to the variable $z_1 = z_\tau$. Eliminating ϕ from the equations (B.4), it can be expressed in terms of Q_τ as

$$z_1 = G(Q_\tau) := \frac{1}{2}\left[1 + f\left(-\sqrt{\frac{-\log Q_\tau}{2} - L^2}\right)\right] . \tag{B.60}$$

Note that $G(Q_0) = z_0$, while

$$G'(Q_0) = -\frac{1}{2Q_0}\frac{1 + f\left(-\sqrt{\frac{-\log Q_0}{2} - L^2}\right)}{f\left(-\sqrt{\frac{-\log Q_0}{2} - L^2}\right)} = \frac{z_0}{Q_0(1-2z_0)} \,, \tag{B.61}$$

and

$$G''(Q) = \frac{1}{2Q^2}\frac{1 + f\left(-\sqrt{\frac{-\log Q}{2} - L^2}\right)}{f\left(-\sqrt{\frac{-\log Q}{2} - L^2}\right)}\left[1 - \frac{1}{f\left(-\sqrt{\frac{-\log Q}{2} - L^2}\right)^2}\right] , \tag{B.62}$$

which has order z_0^2/Q_0^2. The Taylor expansion

$$z_1 = G(Q_0) + (Q_1 - Q_0)G'(Q_0) + \frac{(Q_1 - Q_0)^2}{2}G''(Q_\theta) \tag{B.63}$$

thus becomes

$$z_1 = z_0 + \frac{Q_1 - Q_0}{Q_0}\frac{z_0}{1-2z_0} + \mathcal{O}\left(\left[\frac{Q_1 - Q_0}{Q_0}z_0\right]^2\right) . \tag{B.64}$$

By (B.59), we have

$$\frac{Q_1 - Q_0}{Q_0} = \tilde{\sigma} V_\tau - \tilde{\mu} \frac{w(Q_0, -\phi_0)}{Q_0} + \mathcal{O}\big(\tilde{\mu}^{2(1-\beta)} + \tilde{\sigma}^2 \tilde{\mu}^{-2\beta}\big) \,, \tag{B.65}$$

and Lemma B.3 yields

$$-\mu \frac{w(Q_0, -\phi_0)}{Q_0} = \frac{2\,\mathrm{e}}{L} \Big[Q_0^{-\cos^2 \phi_0} + \mathcal{O}(\log|\log Q_0|) \Big] \Big[1 + \mathcal{O}\Big(\frac{1}{|\log Q_0|} \Big) \Big] \,. \tag{B.66}$$

Now (B.35) implies $Q_0^{-\cos^2 \phi_0} = \mathrm{e}^{2z_0} (2\,\mathrm{e}\, z_0)^{-1}$ and $c_1 |\log z_0| \leqslant |\log Q_0| \leqslant c_2 |\log \tilde{\mu}|$. This completes the proof of the case the case $\sqrt{\varepsilon} \leqslant \tilde{\mu}/|\log \tilde{\mu}|^2$.

In the case $\sqrt{\varepsilon} > \tilde{\mu}/|\log \tilde{\mu}|^2$, we just use the fact that Q_t is bounded below by its value in the previous case, as a consequence of (B.29). □

Corollary B.5. *Assume that either $c = 0$ or $\sqrt{\varepsilon} \leqslant \tilde{\mu}/|\log \tilde{\mu}|^2$. There exists a $\kappa_2 > 0$ such that for an initial condition $(L, z_0) \in F_-$ with $z_0 \geqslant (c_- \tilde{\mu})^{1-\gamma}$, the first hitting of F_+ occurs at a height $z_1 \geqslant z_0$ with probability larger than $1 - \mathrm{e}^{-\kappa_2 \tilde{\mu}^2/\tilde{\sigma}^2}$.*

Proof: It suffices to apply the previous result with $\beta = 1 - \gamma$ and h of order $\tilde{\mu}^\gamma$. □

References

[BAKS84] Gérard Ben Arous, Shigeo Kusuoka, and Daniel W. Stroock, *The Poisson kernel for certain degenerate elliptic operators*, J. Funct. Anal. **56** (1984), no. 2, 171–209.

[BE86] S.M. Baer and T. Erneux, *Singular Hopf bifurcation to relaxation oscillations I*, SIAM J. Appl. Math. **46** (1986), no. 5, 721–739.

[BE92] ———, *Singular Hopf bifurcation to relaxation oscillations II*, SIAM J. Appl. Math. **52** (1992), no. 6, 1651–1664.

[BG02] Nils Berglund and Barbara Gentz, *Pathwise description of dynamic pitchfork bifurcations with additive noise*, Probab. Theory Related Fields **122** (2002), no. 3, 341–388.

[BG09] ———, *Stochastic dynamic bifurcations and excitability*, Stochastic Methods in Neuroscience (Carlo Laing and Gabriel Lord, eds.), Oxford University Press, 2009, pp. 64–93.

[BGK10] Nils Berglund, Barbara Gentz, and Christian Kuehn, *Hunting french ducks in a noisy environment*, `arXiv:1011.3193`, 2010.

[Bir57] Garrett Birkhoff, *Extensions of Jentzsch's theorem*, Trans. Amer. Math. Soc. **85** (1957), 219–227.

[BKLLC11] Peter Borowski, Rachel Kuske, Yue-Xian Li, and Juan Luis Cabrera, *Characterizing mixed mode oscillations shaped by noise and bifurcation structure*, Chaos **20** (2011), no. 4, 043117.

[Bra98] B. Braaksma, *Singular Hopf bifurcation in systems with fast and slow variables*, Journal of Nonlinear Science **8** (1998), no. 5, 457–490.

[Dah77] Björn E. J. Dahlberg, *Estimates of harmonic measure*, Arch. Rational Mech. Anal. **65** (1977), no. 3, 275–288.

[DG11] Susanne Ditlevsen and Priscilla Greenwood, *The Morris–Lecar neuron model embeds a leaky integrate-and-fire model*, Preprint `arXiv:1108.0073`, 2011.

[DGK+11] M. Desroches, J. Guckenheimer, C. Kuehn, B. Krauskopf, H. Osinga, and M. Wechselberger, *Mixed-mode oscillations with multiple time scales*, SIAM Review, in press (2011).

[DT09] Catherine Doss and Michèle Thieullen, *Oscillations and random perturbations of a FitzHugh-Nagumo system*, Preprint hal-00395284 (2009), 2009.

[Fit55] R. FitzHugh, *Mathematical models of threshold phenomena in the nerve membrane*, Bull. Math. Biophysics **17** (1955), 257–269.

[Fit61] R. FitzHugh, *Impulses and physiological states in models of nerve membrane*, Biophys. J. **1** (1961), 445–466.

[HH52] A. L. Hodgkin and A. F. Huxley, *A quantitative description of ion currents and its applications to conduction and excitation in nerve membranes*, J. Physiol. (Lond.) **117** (1952), 500–544.

[HM09] Pawel Hitczenko and Georgi S. Medvedev, *Bursting oscillations induced by small noise*, SIAM J. Appl. Math. **69** (2009), no. 5, 1359–1392.

[Izh00] Eugene M. Izhikevich, *Neural excitability, spiking and bursting*, Internat. J. Bifur. Chaos Appl. Sci. Engrg. **10** (2000), no. 6, 1171–1266.

[Jen12] Robert Jentzsch, *Über Integralgleichungen mit positivem Kern*, J. f. d. reine und angew. Math. **141** (1912), 235–244.

[KP03] Efstratios K. Kosmidis and K. Pakdaman, *An analysis of the reliability phenomenon in the FitzHugh–Nagumo model*, J. Comput. Neuroscience **14** (2003), 5–22.

[KP06] ———, *Stochastic chaos in a neuronal model*, Internat. J. Bifur. Chaos **16** (2006), no. 2, 395–410.

[KR50] M. G. Kreĭn and M. A. Rutman, *Linear operators leaving invariant a cone in a Banach space*, Amer. Math. Soc. Translation **1950** (1950), no. 26, 128.

[LSG99] Benjamin Lindner and Lutz Schimansky-Geier, *Analytical approach to the stochastic FitzHugh-Nagumo system and coherence resonance*, Physical Review E **60** (1999), no. 6, 7270–7276.

[ML81] C. Morris and H. Lecar, *Voltage oscillations in the barnacle giant muscle fiber*, Biophys. J. (1981), 193–213.

[MVE08] Cyrill B. Muratov and Eric Vanden-Eijnden, *Noise-induced mixed-mode oscillations in a relaxation oscillator near the onset of a limit cycle*, Chaos **18** (2008), 015111.

[MVEE05] C.B. Muratov, E. Vanden-Eijnden, and W. E, *Self-induced stochastic resonance in excitable systems*, Physica D **210** (2005), 227–240.

[NAY62] J. S. Nagumo, S. Arimoto, and S. Yoshizawa, *An active pulse transmission line simulating nerve axon*, Proc. IRE **50** (1962), 2061–2070.

[Num84] Esa Nummelin, *General irreducible Markov chains and nonnegative operators*, Cambridge Tracts in Mathematics, vol. 83, Cambridge University Press, Cambridge, 1984.

[Ore71] Steven Orey, *Lecture notes on limit theorems for Markov chain transition probabilities*, Van Nostrand Reinhold Co., London, 1971, Van Nostrand Reinhold Mathematical Studies, No. 34.

[Row07] Peter Rowat, *Interspike interval statistics in the stochastic Hodgkin-Huxley model: Coexistence of gamma frequency bursts and highly irregular firing*, Neural Computation **19** (2007), 12151250.

[SK] David W. J Simpson and Rachel Kuske, *Mixed-mode oscillations in a stochastic, piecewise-linear system*, arXiv:1010.1504 (2010).

[Sow08] Richard B. Sowers, *Random perturbations of canards*, J. Theoret. Probab. **21** (2008), no. 4, 824–889.

[SVJ66] E. Seneta and D. Vere-Jones, *On quasi-stationary distributions in discrete-time Markov chains with a denumerable infinity of states*, J. Appl. Probability **3** (1966), 403–434.

[TGOS08] Marc Turcotte, Jordi Garcia-Ojalvo, and Gurol M. Suel, *A genetic timer through noise-induced stabilization of an unstable state*, PNAS **105** (2008), no. 41, 1573215737.

[TP01a] Seiji Tanabe and K. Pakdaman, *Dynamics of moments of FitzHugh–Nagumo neuronal models and stochastic bifurcations*, Phys. Rev. E **63** (2001), 031911.

[TP01b] Seiji Tanabe and K. Pakdaman, *Noise-induced transition in excitable neuron models*, Biol. Cybern. **85** (2001), 269–280.

[TTP02] Takayuki Takahata, Seiji Tanabe, and K. Pakdaman, *White-noise stimulation of the HodgkinHuxley model*, Biol. Cybern. **86** (2002), 403417.

Contents

Nils Berglund and Damien Landon
Université d'Orléans, Laboratoire Mapmo
CNRS, UMR 6628
Fédération Denis Poisson, FR 2964
Bâtiment de Mathématiques, B.P. 6759
45067 Orléans Cedex 2, France
E-mail address: nils.berglund@univ-orleans.fr, damien.landon@univ-orleans.fr